expression in these 371 patients revealed the prognostic value of pfetin; the metastasis-free survival rate was 93.8% for pfetin-positive patients and 40.6% for pfetin-negative patients ($p < 0.0001$; log-rank test; Fig. 3E) [34]. Using multivariate analyses, we examined clinical and pathological factors that may affect prognosis in GIST patients. These factors included age, gender, site of tumor origin, histology, tumor size, status of necrosis, and risk classification [18, 32–34]. Of these, we determined that risk classification was an independent prognostic factor. Indeed, when the patients were stratified according to risk classification, the prognosis was significantly different among each risk group (Fig. 3F). Notably, the metastasis-free survival curves based on pfetin expression in low-, intermediate-, and high-risk groups were significantly different (Fig. 3G, H, and I, respectively). These observations established pfetin as a prognostic biomarker in GIST. This is the largest and most successful validation study for molecular biomarkers in GIST.

4 Additional biomarker identification, with opposite predictive values to pfetin

In addition to pfetin as a biomarker to predict the favorable prognosis in GIST, we identified a biomarker for unfavorable prognosis. Using 2D-DIGE and surgical specimens, we found that ATP-dependent RNA helicase DDX39 (DDX39) exhibited higher expression level in the GIST patients who developed metastases after surgery [35]. Aberrant expression of DDX39 has been reported in lung squamous cell carcinoma, and in vitro experiments have demonstrated how it contributed to the malignant potential of tumor cells [36,37]. However, there was no data linking DDX39 to GIST. A DDX39 immunohistochemical study confirmed the association of DDX39 with poor prognosis in GIST in 72 patients; the 5-year metastasis-free survival rate was 90.2% (51/72 patients) for DDX39-negative patients and 52.4% (21/72 cases) for DDX39-positive patients ($p < 0.0037$; log-rank test; Fig. 2J) [35]. The combined use of the two biomarkers, pfetin and DDX39, seemed to be effective in the prediction of poor prognosis. Among 72 patients, all ten with pfetin-negative and DDX39-positive tumors had metastases within 2 years after surgery [34]. A validation study with a larger sample size will further establish this application.

5 Lessons from GIST study

We performed proteomic studies with the aim of discovering a prognostic biomarker in GIST, and identified pfetin. We examined 422 GIST cases by immunohistochemistry, and associated overexpression of pfetin with a favorable prognosis. The clinical usefulness of pfetin will continue to be further validated and its functional role in metastasis remains to be investigated. However, this is the largest proteomic approach to sarcoma biomarkers, and a fine example of biomarker discovery by this approach. Thus, it is worth considering what is critically important in biomarker studies in rare diseases, taking our experience as an example.

Firstly, our biomarker study started with only 17 cases. 2D-DIGE experiments require the use of frozen tissues, and the frozen tissues were not routinely stored in the hospital. As a result of this, we had no choice but to begin the biomarker study with a relatively small number of samples. Generally, this number is too small to obtain conclusive biomarker candidates. However, the homogenous molecular background of GIST may make it possible to identify a biomarker candidate even in such conditions. Approximately 80% of GISTs harbor an activating mutation in KIT and 10% in PDGFRA [12], suggesting that the common mechanisms underlying carcinogenesis and development may be generally shared among the cases. Moreover, in our study, no patient received adjuvant therapy with imatinib mesylate [18]. The common molecular and clinical backgrounds may generally result in successful biomarker identification, even when starting with a small number of samples. Several sarcomas are characterized by the presence of common gene mutations. In these sarcomas, we may be able to identify the promising biomarkers even from a small number of samples, if we design the appropriate study. In contrast, we may need a large number of samples to identify biomarker candidates in malignancies with complex molecular backgrounds. Alternatively, we may need to stratify patients according to their genetic status, and create sample groups where only the examined parameters are different between the sample groups.

Secondly, the clinical and pathological factors were extensively considered to estimate the risk of unfavorable prognosis in GIST. These study backgrounds were advantageous in the biomarker study. In addition to the presence or absence of postoperative metastasis, we considered the risk classification, which is based on the size of tumor and the status of mitosis, in the experiment design. When we initially selected the cases and grouped them only according to the status of recurrence, we did not identify pfetin in a comparative study (data not published). Later, we found that 93.9% of the patients with pfetin-positive primary tumors did not have postoperative metastasis, and 63.8% of the patients with pfetin-negative tumors did [18]. Biomarkers with more than 90% prediction values for both sides may be identified even when we only use the data on clinical outcome, such as metastasis post-surgery, but this was not the case for us. When the number of cases in the discovery study is limited, we may select the samples that later turn out to be those not predicted by the intended biomarker. Thus, considering the existing risk classification systems and using these for our study design, we can establish the appropriate study.

Thirdly, the validation study was performed by immunohistochemistry. 2D-DIGE is an excellent method to create protein expression profiles. However, it is not suitable to use as a validation tool, even in laboratories, needless to say, in hospitals, for 2 reasons. Firstly, thousands of protein spots do not have to be observed for validation purposes, and it is a

waste of resources to run 2D-DIGE for only a small number of protein spots. Secondly, 2D-DIGE requires frozen tissues, which are not routinely stored in the hospital, and can be expected only in research-oriented clinical facilities. Although recent reports suggested the possibility that formalin-fixed paraffin-embedded tissue could be used for 2D-DIGE, the number of protein spots reported was much less than when frozen tissues were examined [38,39]. This point raises a problem when carrying out a retrospective validation study in a multi-institutional way. In contrast, immunohistochemistry enables the use of formalin-fixed paraffin-embedded samples. Immunohistochemistry provides valuable information, in terms of not only protein expression level but also protein localization. Indeed, certain biomarkers were effective only when the expression level was considered along with cellular localization [40]. Occasionally, use of the antibodies in immunohistochemistry can be disappointing as they do not always perform as well as expected. However, it is worth trying to optimize the staining conditions and develop antibodies suitable for this procedure. Comprehensive databases such as Human Protein Atlas (http://www.proteinatlas.org/) are useful when considering the practical applications of antibodies.

Fourthly, the clinical significance and expected value of aimed biomarkers were clear in our study. In the clinical setting, prognostic biomarkers have long been required to make the best use of imatinib mesylate in adjuvant treatments in GIST. We can avoid the use of imatinib mesylate in those patients who can be cured by surgery alone. This will prevent the unnecessary risks of possible side effects and save on medical costs. For patients who are predicted to have metastases after surgery, we can consider increasing the dose of imatinib mesylate in the hope of prolonging disease-free survival. Thus, this made it easy to find cooperative doctors for our validation study in a relatively short period of time. The clear purpose of biomarkers was advantageous when the experimental design was considered. There are several technical issues remaining for biomarker discovery, despite the extensive efforts devoted to technology development in the last decade. Whole proteome still cannot be observed in a quantitative way, and for the purpose of clinical examination, the need for this is always demanded and discussed. Although microarray technology for global mRNA expression experiments was established many years ago and has been applied to biomarker studies, the studies are not always successful in all types of malignancies. Therefore, it may not be true that the more comprehensively we observe the proteome, the more likely we are to identify the real biomarker. We employed 2D-DIGE to create protein expression profiles, which uncovers only a limited part of the proteome. We speculate that existing proteomics modalities may reach the level at which the biomarker candidates are obtained, and the use of an adequate sample set with clear clinical purpose is key for successful biomarker studies.

Fifthly, we identified an additional biomarker, DDX39, by increasing the number of observable proteins. We speculate that pfetin is not the only prognostic biomarker, and other candidates should be discovered by different proteomic approaches than 2D-DIGE. Indeed, although our studies are the only ones using the proteomic approach for biomarker discovery in GIST, many prognostic molecular biomarkers were reported in previous genetic and epigenetic studies [41–81]. We may want to finally focus on a single or a few biomarkers for clinical applications, and the appearance of more and more biomarkers may become an obstacle to their practical application. It is a dilemma whether we should continue to try and discover additional biomarkers to go alongside existing ones using novel proteomic approaches, or whether it would be better to focus on the validation of reported biomarker candidates and stop further biomarker discovery by proteomic studies.

Seventhly, the functional significance of pfetin expression in GIST cells is not yet clear. Although the normal functions of pfetin and the association of pfetin with various diseases have been reported elsewhere [3, 24–31], there has been no evidence to support the functional contributions of pfetin to the favorable prognosis in GISTs. It is a general question whether a biomarker should have functional significance. We may need to consider the possibility that pfetin itself does not have a functional role in favorable prognosis in GIST. A particular set of genes whose expression levels are coordinated with pfetin expression may affect the malignant features of GISTs. Recently, ETV1 was reported as a functionally important transcription factor in GIST [82]. The expression of ETV1 was commonly reported in previous global expression studies in GIST, and shown to be specific to GIST over the other malignancies. In vitro experiments demonstrated that ETV1 was regulated by KIT, and promoted cell proliferation and tumor growth. These observations suggested possible clinical utilities of ETV1. However, subsequent studies revealed that ETV1 expression did not correlate with clinical outcome in GIST [83], and we also immunohistochemically confirmed that ETV1 did not have prognostic value in GIST (data not shown). The functional molecule cannot always be the biomarker to assess the malignant features of tumor cells, and the vice versa may also be true.

6 Conclusions

We present our biomarker study for GIST as an example of prognostic biomarker development, and discuss potential key points that could be applicable to other studies. Our study on pfetin in GIST is still underway, but we believe our experience will be useful to other researchers conducting biomarker studies.

We deeply appreciate the clinicians who collaborated with us and provided valuable clinical materials and data; Yasuhiro Shimada, Mitsuru Sasako, Hitoshi Katai, Taketo Okubo, Hajime Orita, and Tatsuo Kanda. We also greatly appreciate the pathologists who performed excellent diagnosis and judgment of the

results of the immunohistochemistry studies; Tadashi Hasegawa, Kunihiko Seki, Naobumi Tochigi, Akihiko Yoshida, and Tsuyoshi Saito. We also thank Prof. Morton for providing us with polyclonal antibody, and Dr. Masahiro Gotoh for his excellent technical support in the generation of the monoclonal antibody. This work was supported by the National Cancer Center Research Core Facility and National Cancer Center Research and Development Fund (23-A-7 and 23-A-10).

The authors have declared no conflict of interest.

7 References

[1] Weiss, S. W., Goldblum, J. R., *Soft Tissue Tumors*, Mosby, Philadelphia, 2007.

[2] Hirota, S., Ohashi, A., Nishida, T., Isozaki, K. et al., Gain-of-function mutations of platelet-derived growth factor receptor alpha gene in gastrointestinal stromal tumors. *Gastroenterology* 2003, *125*, 660–667.

[3] Hirota, S., Isozaki, K., Moriyama, Y., Hashimoto, K. et al., Gain-of-function mutations of c-kit in human gastrointestinal stromal tumors. *Science* 1998, *279*, 577–580.

[4] Heinrich, M. C., Corless, C. L., Duensing, A., McGreevey, L. et al., PDGFRA activating mutations in gastrointestinal stromal tumors. *Science* 2003, *299*, 708–710.

[5] Versteege, I., Sevenet, N., Lange, J., Rousseau-Merck, M. F. et al., Truncating mutations of hSNF5/INI1 in aggressive paediatric cancer. *Nature* 1998, *394*, 203–206.

[6] Fritz, B., Schubert, F., Wrobel, G., Schwaenen, C. et al., Microarray-based copy number and expression profiling in dedifferentiated and pleomorphic liposarcoma. *Cancer Res.* 2002, *62*, 2993–2998.

[7] Quesada, J., Amato, R., The molecular biology of soft-tissue sarcomas and current trends in therapy. *Sarcoma* 2012, *2012*, 849456.

[8] Oda, Y., Tsuneyoshi, M., Recent advances in the molecular pathology of soft tissue sarcoma: implications for diagnosis, patient prognosis, and molecular target therapy in the future. *Cancer Sci.* 2009, *100*, 200–208.

[9] Joensuu, H., Roberts, P. J., Sarlomo-Rikala, M., Andersson, L. C. et al., Effect of the tyrosine kinase inhibitor STI571 in a patient with a metastatic gastrointestinal stromal tumor. *N. Engl. J. Med.* 2001, *344*, 1052–1056.

[10] Joensuu, H., Vehtari, A., Riihimaki, J., Nishida, T. et al., Risk of recurrence of gastrointestinal stromal tumour after surgery: an analysis of pooled population-based cohorts. *Lancet Oncol.* 2012, *13*, 265–274.

[11] Erkizan, H. V., Kong, Y., Merchant, M., Schlottmann, S. et al., A small molecule blocking oncogenic protein EWS-FLI1 interaction with RNA helicase A inhibits growth of Ewing's sarcoma. *Nat. Med.* 2009, *15*, 750–756.

[12] Rubin, B. P., Heinrich, M. C., Corless, C. L., Gastrointestinal stromal tumour. *Lancet* 2007, *369*, 1731–1741.

[13] Kawanowa, K., Sakuma, Y., Sakurai, S., Hishima, T. et al., High incidence of microscopic gastrointestinal stromal tumors in the stomach. *Hum. Pathol.* 2006, *37*, 1527–1535.

[14] Agaimy, A., Wunsch, P. H., Hofstaedter, F., Blaszyk, H. et al., Minute gastric sclerosing stromal tumors (GIST tumorlets) are common in adults and frequently show c-KIT mutations. *Am. J. Surg. Pathol.* 2007, *31*, 113–120.

[15] Dagher, R., Cohen, M., Williams, G., Rothmann, M. et al., Approval summary: imatinib mesylate in the treatment of metastatic and/or unresectable malignant gastrointestinal stromal tumors. *Clin. Cancer Res.* 2002, *8*, 3034–3038.

[16] Joensuu, H., Eriksson, M., Sundby Hall, K., Hartmann, J. T. et al., One vs three years of adjuvant imatinib for operable gastrointestinal stromal tumor: a randomized trial. *JAMA* 2012, *307*, 1265–1272.

[17] Comparison of two doses of imatinib for the treatment of unresectable or metastatic gastrointestinal stromal tumors: a meta-analysis of 1,640 patients. *J. Clin. Oncol.* 2010, *28*, 1247–1253.

[18] Suehara, Y., Kondo, T., Seki, K., Shibata, T. et al., Pfetin as a prognostic biomarker of gastrointestinal stromal tumors revealed by proteomics. *Clin. Cancer Res.* 2008, *14*, 1707–1717.

[19] Kondo, T., Kubota, D., Kawai, A., Application of proteomics to soft tissue sarcomas. *Int. J. Proteomics* 2012, *2012*, 876401.

[20] Suehara, Y., Kondo, T., Fujii, K., Hasegawa, T. et al., Proteomic signatures corresponding to histological classification and grading of soft-tissue sarcomas. *Proteomics* 2006, *6*, 4402–4409.

[21] Hasegawa, T., Matsuno, Y., Shimoda, T., Hirohashi, S., Gastrointestinal stromal tumor: consistent CD117 immunostaining for diagnosis, and prognostic classification based on tumor size and MIB-1 grade. *Hum. Pathol.* 2002, *33*, 669–676.

[22] Unlu, M., Morgan, M. E., Minden, J. S., Difference gel electrophoresis: a single gel method for detecting changes in protein extracts. *Electrophoresis* 1997, *18*, 2071–2077.

[23] Shaw, J., Rowlinson, R., Nickson, J., Stone, T. et al., Evaluation of saturation labelling two-dimensional difference gel electrophoresis fluorescent dyes. *Proteomics* 2003, *3*, 1181–1195.

[24] Resendes, B. L., Kuo, S. F., Robertson, N. G., Giersch, A. B. et al., Isolation from cochlea of a novel human intronless gene with predominant fetal expression. *J. Assoc. Res. Otolaryngol.* 2004, *5*, 185–202.

[25] Gamse, J. T., Thisse, C., Thisse, B., Halpern, M. E., The parapineal mediates left-right asymmetry in the zebrafish diencephalon. *Development* 2003, *130*, 1059–1068.

[26] Aizawa, H., Goto, M., Sato, T., Okamoto, H., Temporally regulated asymmetric neurogenesis causes left-right difference in the zebrafish habenular structures. *Dev. Cell* 2007, *12*, 87–98.

[27] Cauchi, S., Proenca, C., Choquet, H., Gaget, S. et al., Analysis of novel risk loci for type 2 diabetes in a general French population: the D.E.S.I.R. study. *J. Mol. Med. (Berl)* 2008, *86*, 341–348.

[28] Lee, M. T., Chen, C. H., Lee, C. S., Chen, C. C. et al., Genome-wide association study of bipolar I disorder in the Han Chinese population. *Mol. Psychiatry* 2011, *16*, 548–556.

[29] Metz, M., Gassmann, M., Fakler, B., Schaeren-Wiemers, N., Bettler, B., Distribution of the auxiliary GABAB receptor

subunits KCTD8, 12, 12b, and 16 in the mouse brain. *J. Comp. Neurol.* 2011, *519*, 1435–1454.

[30] Hayasaki, H., Sohma, Y., Kanbara, K., Otsuki, Y., Heterogenous GABA(B) receptor-mediated pathways are involved in the local GABAergic system of the rat trigeminal ganglion: possible involvement of KCTD proteins. *Neuroscience* 2012, *218*, 344–358.

[31] Sand, P. G., Langguth, B., Itzhacki, J., Bauer, A. et al., Resequencing of the auxiliary GABA(B) receptor subunit gene KCTD12 in chronic tinnitus. *Front Syst. Neurosci.* 2012, *6*, 41.

[32] Kikuta, K., Gotoh, M., Kanda, T., Tochigi, N. et al., Pfetin as a prognostic biomarker in gastrointestinal stromal tumor: novel monoclonal antibody and external validation study in multiple clinical facilities. *Jpn. J. Clin. Oncol.* 2010, *40*, 60–72.

[33] Kubota, D., Orita, H., Yoshida, A., Gotoh, M. et al., Pfetin as a prognostic biomarker for gastrointestinal stromal tumor: validation study in multiple clinical facilities. *Jpn. J. Clin. Oncol.* 2011, *41*, 1194–1202.

[34] Kubota, D., Okubo, T., Saito, T., Suehara, Y. et al., Validation study on pfetin and ATP-dependent RNA helicase DDX39 as prognostic biomarkers in gastrointestinal stromal tumour. *Jpn. J. Clin. Oncol.* 2012.

[35] Kikuta, K., Kubota, D., Saito, T., Orita, H. et al., Clinical proteomics identified ATP-dependent RNA helicase DDX39 as a novel biomarker to predict poor prognosis of patients with gastrointestinal stromal tumor. *J. Proteomics* 2012, *75*, 1089–1098.

[36] Sugiura, T., Nagano, Y., Noguchi, Y., DDX39, upregulated in lung squamous cell cancer, displays RNA helicase activities and promotes cancer cell growth. *Cancer Biol. Ther.* 2007, *6*, 957–964.

[37] Sugiura, T., Sakurai, K., Nagano, Y., Intracellular characterization of DDX39, a novel growth-associated RNA helicase. *Exp. Cell Res.* 2007, *313*, 782–790.

[38] Tanca, A., Pagnozzi, D., Falchi, G., Tonelli, R. et al., Application of 2-D DIGE to formalin-fixed, paraffin-embedded tissues. *Proteomics* 2011, *11*, 1005–1011.

[39] Kahler, D., Alexander, C., Schultz, H., Abdullah, M. et al., Proteomics out of the archive: two-dimensional electrophoresis and mass spectrometry using HOPE-fixed, paraffin-embedded tissues. *J. Histochem. Cytochem.* 2010, *58*, 221–228.

[40] Sugihara, Y., Taniguchi, H., Kushima, R., Tsuda, H. et al., Proteomic-based identification of the APC-binding protein EB1 as a candidate of novel tissue biomarker and therapeutic target for colorectal cancer. *J. Proteomics* 2012.

[41] Edris, B., Espinosa, I., Muhlenberg, T., Mikels, A. et al., ROR2 is a novel prognostic biomarker and a potential therapeutic target in leiomyosarcoma and gastrointestinal stromal tumour. *J. Pathol.* 2012.

[42] Niinuma, T., Suzuki, H., Nojima, M., Nosho, K. et al., Upregulation of miR-196a and HOTAIR drive malignant character in gastrointestinal stromal tumors. *Cancer Res.* 2012, *72*, 1126–1136.

[43] Fujita, A., Yamamoto, H., Imamura, M., Nakamura, N. et al., Expression level of the mitotic checkpoint protein and G2-M cell cycle regulators and prognosis in gastrointestinal stromal tumors in the stomach. *Virchows Arch.* 2012, *460*, 163–169.

[44] Okamoto, Y., Sawaki, A., Ito, S., Nishida, T. et al., Aberrant DNA methylation associated with aggressiveness of gastrointestinal stromal tumour. *Gut* 2012, *61*, 392–401.

[45] Zander, H., Rawnaq, T., von Wedemeyer, M., Tachezy, M. et al., Circulating levels of cell adhesion molecule L1 as a prognostic marker in gastrointestinal stromal tumor patients. *BMC Cancer* 2011, *11*, 189:181–187.

[46] Wozniak, A., Rutkowski, P., Piskorz, A., Ciwoniuk, M. et al., Prognostic value of KIT/PDGFRA mutations in gastrointestinal stromal tumours (GIST): Polish Clinical GIST Registry experience. *Ann. Oncol.* 2012, *23*, 353–360.

[47] Setoguchi, T., Kikuchi, H., Yamamoto, M., Baba, M. et al., Microarray analysis identifies versican and CD9 as potent prognostic markers in gastric gastrointestinal stromal tumors. *Cancer Sci.* 2011, *102*, 883–889.

[48] Ruiz-Tovar, J., Diez-Tabernilla, M., Housari, G., Martinez-Molina, E., Sanjuanbenito, A., Gastrointestinal stromal tumors: actin expression, a new prognostic factor? *Am. Surg.* 2010, *76*, 1244–1250.

[49] Arne, G., Kristiansson, E., Nerman, O., Kindblom, L. G. et al., Expression profiling of GIST: CD133 is associated with KIT exon 11 mutations, gastric location and poor prognosis. *Int. J. Cancer* 2011, *129*, 1149–1161.

[50] Braggio, E., Braggio Dde, A., Small, I. A., Lopes, L. F. et al., Prognostic relevance of KIT and PDGFRA mutations in gastrointestinal stromal tumors. *Anticancer Res.* 2010, *30*, 2407–2414.

[51] Rawnaq, T., Kunkel, M., Bachmann, K., Simon, R. et al., Serum midkine correlates with tumor progression and imatinib response in gastrointestinal stromal tumors. *Ann. Surg. Oncol.* 2011, *18*, 559–565.

[52] Hsu, K. H., Tsai, H. W., Lin, P. W., Hsu, Y. S. et al., Osteopontin expression is an independent adverse prognostic factor in resectable gastrointestinal stromal tumor and its interaction with CD44 promotes tumor proliferation. *Ann. Surg. Oncol.* 2010, *17*, 3043–3052.

[53] Hsu, K. H., Tsai, H. W., Lin, P. W., Hsu, Y. S. et al., Clinical implication and mitotic effect of CD44 cleavage in relation to osteopontin/CD44 interaction and dysregulated cell cycle protein in gastrointestinal stromal tumor. *Ann. Surg. Oncol.* 2010, *17*, 2199–2212.

[54] Silva, M., Veiga, I., Ribeiro, F. R., Vieira, J. et al., Chromosome copy number changes carry prognostic information independent of KIT/PDGFRA point mutations in gastrointestinal stromal tumors. *BMC Med.* 2010, *8*, 26.

[55] Martinho, O., Gouveia, A., Silva, P., Pimenta, A. et al., Loss of RKIP expression is associated with poor survival in GISTs. *Virchows Arch.* 2009, *455*, 277–284.

[56] Rawnaq, T., Schwarzenbach, H., Schurr, P. G., Freise, K. et al., Monitoring of loss of heterozygosity in serum microsatellite DNA among patients with gastrointestinal stromal tumors indicates tumor recurrence. *J. Surg. Res.* 2011, *169*, 31–35.

[57] Wei, Y. C., Li, C. F., Yu, S. C., Chou, F. F. et al., Ezrin overexpression in gastrointestinal stromal tumors: an independent

adverse prognosticator associated with the non-gastric location. *Mod. Pathol.* 2009, *22*, 1351–1360.

[58] Song, Z., Wang, J. L., Pan, Y. L., Tao, D. Y. et al., Survival and prognostic factors analysis in surgically resected gastrointestinal stromal tumor patients. *Hepatogastroenterology* 2009, *56*, 149–153.

[59] Hou, Y. Y., Grabellus, F., Weber, F., Zhou, Y. et al., Impact of KIT and PDGFRA gene mutations on prognosis of patients with gastrointestinal stromal tumors after complete primary tumor resection. *J. Gastrointest Surg.* 2009, *13*, 1583–1592.

[60] Yamaguchi, U., Nakayama, R., Honda, K., Ichikawa, H. et al., Distinct gene expression-defined classes of gastrointestinal stromal tumor. *J. Clin. Oncol.* 2008, *26*, 4100–4108.

[61] Perez, D., Herrmann, T., Jungbluth, A. A., Samartzis, P. et al., Cancer testis antigen expression in gastrointestinal stromal tumors: new markers for early recurrence. *Int. J. Cancer* 2008, *123*, 1551–1555.

[62] Mearadji, A., den Bakker, M. A., van Geel, A. N., Eggermont, A. M. et al., Decrease of CD117 expression as possible prognostic marker for recurrence in the resected specimen after imatinib treatment in patients with initially unresectable gastrointestinal stromal tumors: a clinicopathological analysis. *Anticancer Drugs* 2008, *19*, 607–612.

[63] Braconi, C., Bracci, R., Bearzi, I., Bianchi, F. et al., KIT and PDGFRalpha mutations in 104 patients with gastrointestinal stromal tumors (GISTs): a population-based study. *Ann. Oncol.* 2008, *19*, 706–710.

[64] Perez, D., Demartines, N., Meier, K., Clavien, P. A. et al., Protein S100 as prognostic marker for gastrointestinal stromal tumors: a clinicopathological risk factor analysis. *J. Invest Surg.* 2007, *20*, 181–186.

[65] Takeyama, H., Funahashi, H., Sawai, H., Takahashi, H. et al., Expression of alpha6 integrin subunit is associated with malignancy in gastric gastrointestinal stromal tumors. *Med. Sci. Monit.* 2007, *13*, CR51–56.

[66] Kaifi, J. T., Fiegel, H. C., Rafnsdottir, S. L., Aridome, K. et al., Midkine as a prognostic marker for gastrointestinal stromal tumors. *J. Cancer Res. Clin. Oncol.* 2007, *133*, 431–435.

[67] Huang, H. Y., Huang, W. W., Lin, C. N., Eng, H. L. et al., Immunohistochemical expression of p16INK4A, Ki-67, and Mcm2 proteins in gastrointestinal stromal tumors: prognostic implications and correlations with risk stratification of NIH consensus criteria. *Ann. Surg. Oncol.* 2006, *13*, 1633–1644.

[68] Kaifi, J. T., Wagner, M., Schurr, P. G., Wachowiak, R. et al., Allelic loss of Hox11L1 gene locus predicts outcome of gastrointestinal stromal tumors. *Oncol. Rep.* 2006, *16*, 915–919.

[69] Schurr, P., Wolter, S., Kaifi, J., Reichelt, U. et al., Microsatellite DNA alterations of gastrointestinal stromal tumors are predictive for outcome. *Clin. Cancer Res.* 2006, *12*, 5151–5157.

[70] Andersson, J., Bumming, P., Meis-Kindblom, J. M., Sihto, H. et al., Gastrointestinal stromal tumors with KIT exon 11 deletions are associated with poor prognosis. *Gastroenterology* 2006, *130*, 1573–1581.

[71] Cho, S., Kitadai, Y., Yoshida, S., Tanaka, S. et al., Deletion of the KIT gene is associated with liver metastasis and poor prognosis in patients with gastrointestinal stromal tumor in the stomach. *Int. J. Oncol.* 2006, *28*, 1361–1367.

[72] Steinert, D. M., Oyarzo, M., Wang, X., Choi, H. et al., Expression of Bcl-2 in gastrointestinal stromal tumors: correlation with progression-free survival in 81 patients treated with imatinib mesylate. *Cancer* 2006, *106*, 1617–1623.

[73] Haller, F., Gunawan, B., von Heydebreck, A., Schwager, S. et al., Prognostic role of E2F1 and members of the CDKN2A network in gastrointestinal stromal tumors. *Clin. Cancer Res.* 2005, *11*, 6589–6597.

[74] Martin, J., Poveda, A., Llombart-Bosch, A., Ramos, R. et al., Deletions affecting codons 557–558 of the c-KIT gene indicate a poor prognosis in patients with completely resected gastrointestinal stromal tumors: a study by the Spanish Group for Sarcoma Research (GEIS). *J. Clin. Oncol.* 2005, *23*, 6190–6198.

[75] Nakamura, N., Yamamoto, H., Yao, T., Oda, Y. et al., Prognostic significance of expressions of cell-cycle regulatory proteins in gastrointestinal stromal tumor and the relevance of the risk grade. *Hum. Pathol.* 2005, *36*, 828–837.

[76] Chen, W. T., Huang, C. J., Wu, M. T., Yang, S. F. et al., Hypoxia-inducible factor-1alpha is associated with risk of aggressive behavior and tumor angiogenesis in gastrointestinal stromal tumor. *Jpn. J. Clin. Oncol.* 2005, *35*, 207–213.

[77] Kim, T. W., Lee, H., Kang, Y. K., Choe, M. S. et al., Prognostic significance of c-kit mutation in localized gastrointestinal stromal tumors. *Clin. Cancer Res.* 2004, *10*, 3076–3081.

[78] Montgomery, E., Abraham, S. C., Fisher, C., Deasel, M. R. et al., CD44 loss in gastric stromal tumors as a prognostic marker. *Am. J. Surg. Pathol.* 2004, *28*, 168–177.

[79] Kanat, O., Adim, S., Evrensel, T., Yerci, O. et al., Prognostic value of nm23 in gastrointestinal stromal tumors. *Med. Oncol.* 2004, *21*, 53–58.

[80] Takahashi, R., Tanaka, S., Hiyama, T., Ito, M. et al., Hypoxia-inducible factor-1alpha expression and angiogenesis in gastrointestinal stromal tumor of the stomach. *Oncol. Rep.* 2003, *10*, 797–802.

[81] Toquet, C., Le Neel, J. C., Guillou, L., Renaudin, K. et al., Elevated (> or = 10%) MIB-1 proliferative index correlates with poor outcome in gastric stromal tumor patients: a study of 35 cases. *Dig. Dis. Sci.* 2002, *47*, 2247–2253.

[82] Chi, P., Chen, Y., Zhang, L., Guo, X. et al., ETV1 is a lineage survival factor that cooperates with KIT in gastrointestinal stromal tumours. *Nature* 2010, *467*, 849–853.

[83] Birner, P., Beer, A., Vinatzer, U., Stary, S. et al., MAP-KAP kinase 2 overexpression influences prognosis in gastrointestinal stromal tumors and associates with copy number variations on chromosome 1 and expression of p38 MAP kinase and ETV1. *Clin. Cancer Res.* 2012, *18*, 1879–1887.

Oncogene (2013), 1–11

www.nature.com/onc

ORIGINAL ARTICLE

SS18-SSX fusion protein-induced Wnt/β-catenin signaling is a therapeutic target in synovial sarcoma

M Trautmann[1,2], E Sievers[1], S Aretz[3], D Kindler[1], S Michels[1], N Friedrichs[1], M Renner[4], J Kirfel[2], S Steiner[2], S Huss[1], A Koch[5], R Penzel[4], O Larsson[6], A Kawai[7], S Tanaka[8], H Sonobe[9], A Waha[10], P Schirmacher[4], G Mechtersheimer[4], E Wardelmann[1], R Büttner[1] and W Hartmann[1]

Synovial sarcoma is a high-grade soft tissue malignancy characterized by a specific reciprocal translocation t(X;18), which leads to the fusion of the *SS18* (*SYT*) gene to one of three *SSX* genes (*SSX1*, *SSX2* or *SSX4*). The resulting chimeric SS18-SSX protein is suggested to act as an oncogenic transcriptional regulator. Despite multimodal therapeutic approaches, metastatic disease is often lethal and the development of novel targeted therapeutic strategies is required. Several expression-profiling studies identified distinct gene expression signatures, implying a consistent role of Wnt/β-catenin signaling in synovial sarcoma tumorigenesis. Here we investigate the functional and therapeutic relevance of Wnt/β-catenin pathway activation *in vitro* and *in vivo*. Immunohistochemical analyses of nuclear β-catenin and Wnt downstream targets revealed activation of canonical Wnt signaling in a significant subset of 30 primary synovial sarcoma specimens. Functional aspects of Wnt signaling including dependence of Tcf/β-catenin complex activity on the SS18-SSX fusion proteins were analyzed. Efficient SS18-SSX-dependent activation of the Tcf/β-catenin transcriptional complex was confirmed by TOPflash reporter luciferase assays and immunoblotting. In five human synovial sarcoma cell lines, inhibition of the Tcf/β-catenin protein–protein interaction significantly blocked the canonical Wnt/β-catenin signaling cascade, accompanied by the effective downregulation of Wnt targets (AXIN2, CDC25A, c-MYC, DKK1, CyclinD1 and Survivin) and the specific suppression of cell viability associated with the induction of apoptosis. In SYO-1 synovial sarcoma xenografts, administration of small molecule Tcf/β-catenin complex inhibitors significantly reduced tumor growth, associated with diminished AXIN2 protein levels. In summary, SS18-SSX-induced Wnt/β-catenin signaling appears to be of crucial biological importance in synovial sarcoma tumorigenesis and progression, representing a potential molecular target for the development of novel therapeutic strategies.

Oncogene advance online publication, 28 October 2013; doi:10.1038/onc.2013.443

Keywords: Synovial sarcoma; SYT-SSX; β-catenin; Wnt signaling pathway; PKF115-584; CGP049090; PKF118-310

INTRODUCTION

Synovial sarcoma is an aggressive malignancy comprising ~7–10% of all soft tissue tumors with a predominance in adolescents and young adults.[1] The molecular hallmark of synovial sarcoma is a pathognomonic reciprocal translocation t(X;18)(p11;q11), leading to the fusion of *SS18* (*SYT*) to one of the homologs *SSX* genes (most frequently *SSX1* or *SSX2*, in rare cases *SSX4*), generating oncogenic SS18-SSX chimeric proteins.[2–4] Although the pathognomonic SS18-SSX fusion proteins seem to have a crucial role in synovial sarcoma tumorigenesis and progression, the specific biological function and the mechanism of action remain to be defined. Neither SS18, the SSX proteins, nor the chimeric SS18-SSX oncoproteins have known DNA-binding motifs; however, they have been reported to contribute to the dysregulation of gene expression through association with SWI/SNF and Polycomb chromatin remodeling complexes.[5–8] On the basis of several microarray expression-profiling studies, one of the pathways recurrently found deregulated in synovial sarcoma is the Wnt/β-catenin signaling pathway.[9–13]

Wnt/β-catenin signaling has fundamental roles in the regulation of diverse biological processes, including embryogenesis, cell proliferation, survival and tissue regeneration. The central key mediator of the canonical Wnt pathway is β-catenin, which is, as long as the pathway is inactive, degraded through a multiprotein complex including axis inhibition protein (AXIN), adenomatous polyposis coli (APC), casein-kinase-1 (CK1) and glycogen synthase kinase-3beta (GSK-3β). Upon activation of the signaling cascade by binding of Wnt ligands to frizzled receptors (FZD), the multiprotein destruction complex is disrupted and β-catenin translocates to the nucleus, where it interacts with transcription factors of the T-cell factor (Tcf) and lymphoid enhancer factor (Lef) family inducing expression of downstream targets, including AXIN2, CDC25A, c-MYC, DKK1, CyclinD1 and Survivin.[14,15] Increasing evidence suggests that aberrant activation of Wnt/β-catenin signaling is associated with tumor development and progression in various types of cancer.[16–18] In a variety of malignancies, oncogenic pathway activation is derived from genetic alterations in central signaling components, including *β-catenin* and *APC*. In synovial

[1]Department of Pathology, University Hospital Cologne, Cologne, Germany; [2]Department of Pathology, University Hospital Bonn, Bonn, Germany; [3]Institute of Human Genetics, University of Bonn, Bonn, Germany; [4]Department of Pathology, University Hospital Heidelberg, Heidelberg, Germany; [5]Department of Neuropathology, Charité-Universitätsmedizin, Berlin, Germany; [6]Departments of Oncology & Pathology, The Karolinska Institute, Stockholm, Sweden; [7]Division of Orthopaedic Surgery, National Cancer Center Hospital, Tokyo, Japan; [8]Laboratory of Molecular & Cellular Pathology, Hokkaido University Graduate School of Medicine, Sapporo, Japan; [9]Department of Laboratory Medicine, Chungoku Central Hospital, Fukuyama, Hiroshima, Japan and [10]Department of Neuropathology, University Hospital Bonn, Bonn, Germany. Correspondence: Dr W Hartmann, Department of Pathology, University Hospital Cologne, Kerpener Str. 62, 50937 Cologne, Germany.
E-mail: wolfgang.hartmann@uk-koeln.de
Received 10 April 2013; revised 11 September 2013; accepted 16 September 2013

sarcoma, oncogenic mutations of Wnt pathway components have been reported in a minor frequency,[19–21] suggesting a functional key role of the SS18-SSX chimeric oncoprotein.

The objective of the present study is to explore the functional relevance of Wnt/β-catenin signaling in synovial sarcoma tumorigenesis including its molecular dependence on the pathognomonic SS18-SSX fusion proteins and to preclinically test novel molecularly targeted approaches employing small molecule inhibitors of the Tcf/β-catenin protein complex.[22–24]

RESULTS

Expression of Wnt/β-catenin signaling components in primary synovial sarcoma and tumor-derived cell lines

To determine the involvement of Wnt/β-catenin signaling in synovial sarcoma tumorigenesis, the expressions of nuclear β-catenin and Wnt targets were examined in a set of 30 primary synovial sarcoma specimens by immunohistochemical analysis. Significant nuclear staining of β-catenin was found in 73% (22/30) of cases (Figure 1a). Five out of 30 tumors (17%) showed no

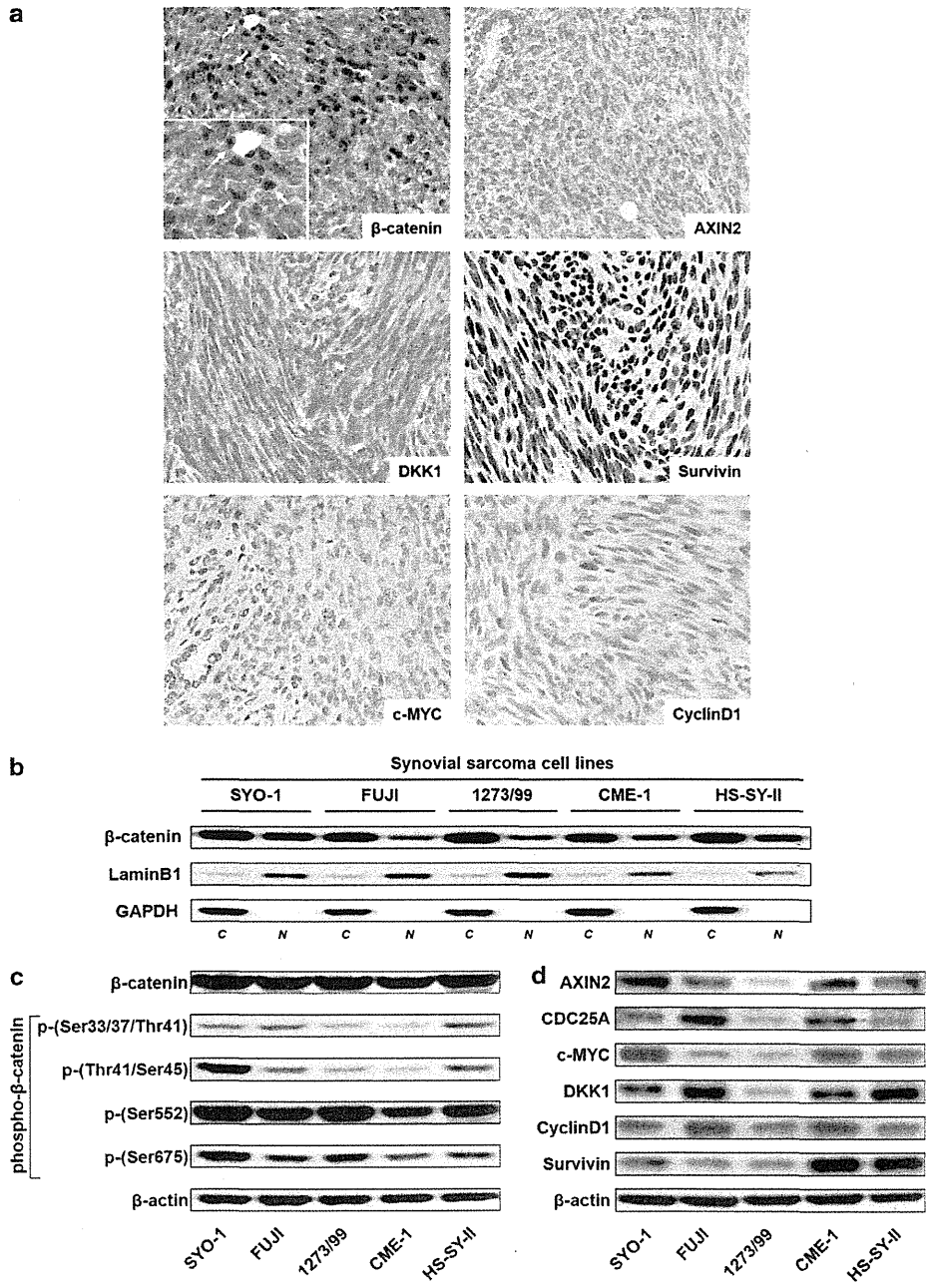

Figure 1. Activation of Wnt/β-catenin signaling in synovial sarcoma. (**a**) Immunohistochemical stainings showing nuclear localization of β-catenin and expression of Wnt/β-catenin targets in a representative case of synovial sarcoma (original magnification: × 20, inset × 40). (**b**) Detection of the cytoplasmic (C) and nuclear (N) fractions of β-catenin in five synovial sarcoma cell lines, nuclear localization being an indicator of pathway activity. GAPDH and LaminB1 were used as controls for the cytoplasmic and nuclear fractions, respectively. (**c**) Immunoblotting for phospho-β-catenin in synovial sarcoma cell lines. (**d**) Elevated expression levels of Wnt signaling targets in total protein extracts of synovial sarcoma cell lines.

nuclear β-catenin immunoreactivity. Consistently, several Wnt targets were highly expressed in synovial sarcoma including AXIN2, DKK1, Survivin, c-MYC and CyclinD1 (Figure 1a). In all, 63% of the tumors displayed strong expression levels of AXIN2 and 37% showed weak expression. DKK1 was strongly expressed in 40% (12/30) of cases, weakly in 57% (17/30) and, in only a single case, no DKK1 expression was detectable. Strong expression of Survivin was detectable in all tumor samples. Expression levels for c-MYC were strong in 30% of the samples, weak in 27% and 43% of the tumors were negative for c-MYC. In concordance, c-MYC-negative tumor samples showed lower β-catenin nuclear staining scores compared with c-MYC-positive cases. Strong expression of CyclinD1 was detected in 32% of the tumors, 25% of the samples displayed weak expression levels and 12 tumors did not show any expression of CyclinD1. There was a significant overlap of nuclear β-catenin immunoreactivity and the strong expression of at least two Wnt targets in 23 out of 25 tumors (92%). However, distinct cases (5/30) displayed target expression without evidence of nuclear β-catenin accumulation, pointing to a more elaborate regulatory context. Expression of Wnt target genes did not correlate with the patients' age, gender, the translocation subtype or tumor size (Figure 1 and Supplementary Table S1).

In accordance with the immunohistochemical results in primary tumor tissues, elevated β-catenin protein levels were found in nuclear extracts and immunostainings of synovial sarcoma cell lines, corresponding to the transcriptionally active pool of β-catenin (Figure 1b and data not shown). MCF-7 breast carcinoma cells (known to have an activated Wnt/β-catenin signaling cascade) and MDA-MB-453 (showing only very faint nuclear levels of β-catenin) were included as controls (Supplementary Figure S1).[25,26] The fraction of β-catenin phosphorylated at Ser45, Ser33, Ser37 and Thr41 (all destabilizing phosphorylation steps exerted by CK1 and GSK-3β)[27] was low compared with the fraction of β-catenin phosphorylated at Ser552 and Ser675 (inducing β-catenin accumulation in the nucleus)[28] (Figure 1c). Indeed, protein levels of Wnt signaling target genes were elevated in all but one synovial sarcoma cell line (Figure 1d).

As mutations in *CTNNB1* (encoding β-catenin) or *APC* might be responsible for Wnt/β-catenin pathway activation, we screened the *CTNNB1* exon 3 sequence (encoding the regulatory degradation targeting box of β-catenin) and the entire *APC* coding region for mutations. All synovial sarcoma cell lines were wild type for *APC*, and none of them displayed mutations in the regulatory phospho-sites of the degradation targeting box of β-catenin. In SYO-1 cells, we detected a p.G34L point mutation (*CTNNB1*). Alterations in codon 34 have been reported to lack transforming transcriptional activation potential.[29]

Activation of Wnt/β-catenin signaling is induced by SS18-SSX

To evaluate whether Tcf/β-catenin transcriptional activity is molecularly dependent on the SS18-SSX fusion proteins, HEK293 cells were transfected with *SS18-SSX1, SS18-SSX2, SS18, SSX1* and *SSX2* expression plasmids. In luciferase reporter assays employing the TOP-/FOPflash system, expression of *SS18-SSX* significantly increased TOPflash reporter activity by 15- to 20-fold compared with *SS18, SSX1, SSX2* or the mutant ΔN131 β-catenin[30] control (Figure 2a). We next determined the functional requirement of β-catenin for SS18-SSX-induced TOPflash reporter activity. Knockdown of β-catenin by small interfering RNA (siRNA) significantly reduced the TOPflash reporter activity enhanced by SS18-SSX1 and SS18-SSX2 (Figure 2c). These results suggest that β-catenin is required for SS18-SSX-associated induction of Tcf/β-catenin-mediated transcriptional activity. In agreement with published results,[31] expression of SS18-SSX or mutant ΔN131 β-catenin induced nuclear recruitment and accumulation of β-catenin (Supplementary Figure S2). In contrast, no changes in cellular localization of β-catenin were detected in cells transient transfected with *SS18, SSX1* or *SSX2*.

Comparable to what has been observed in NIH3T3 cells,[31] the induction of Wnt target expression in HEK293 cells upon SS18-SSX expression was rather weak though TOP-Flash assays indicated a strong activation of β-catenin/TCF transcriptional activity. We therefore chose HT1080 fibrosarcoma cells as an additional *in vitro* model to further investigate the expression of Wnt/β-catenin signaling downstream targets, as these cells have been reported to express nuclear β-catenin at low levels, indicating basal pathway activity.[17] Immunoblot analyses showed elevated levels of AXIN2, CDC25A, DKK1 and CyclinD1 upon expression of the SS18-SSX fusion proteins (Figure 2b). Destabilizing phosphorylation of β-catenin at residues Ser45, Ser33, Ser37 and Thr41 remained constant. Likewise, no relevant changes in the fraction of β-catenin phosphorylated at Ser552 and Ser675 were found (data not shown).

PKF115–584, CGP049090 and PKF118–310 suppress cell viability of synovial sarcoma cell lines *in vitro*

To investigate the biological effects of treatment with small molecule inhibitors of the Tcf/β-catenin complex (PKF115–584, CGP049090 and PKF118–310), synovial sarcoma and control cell lines (MCF-7 and MDA-MB-453) were exposed to increasing concentrations (0.15–1.25 μM) of these compounds for 72 h. All three substances were effective in reducing synovial sarcoma and MCF-7 cell viability with IC_{50} values ranging from 0.17– to 1.82 μM (Figure 3a and Table 1). SYO-1, CME-1 and HS-SY-II cells were more sensitive to treatment compared with FUJI and 1273/99 cells, but no correlation between the SS18-SSX translocation subtype and the exerted effect was observed. IC_{50} values of synovial sarcoma cell lines were comparable to those of MCF-7 control cells with known activation of Wnt/β-catenin signaling and similar to previously reported IC_{50} values in colon and prostate cancer cell lines.[22] In contrast, MDA-MB-453 control cells with almost undetectable nuclear levels of β-catenin showed only minor responses. These results argue in favor of Wnt/β-catenin specificity of the substances' mode of action. Combination of Tcf/β-catenin complex inhibition with conventional chemotherapeutic agents (Vincristine, Doxorubicin and Actinomycin D; 0.1–1000 ng/ml) resulted in additive effects on SYO-1 cell viability (Figure 3b).

PKF115–584, CGP049090 and PKF118–310 inhibit Tcf/β-catenin interaction and mediated transcriptional activity

Effects of treatment with PKF115–584, CGP049090 and PKF118–310 on Tcf/β-catenin-mediated transcriptional activity in synovial sarcoma cell lines were assessed employing the TOP-/FOPflash luciferase reporter assay. Significant dose-dependent (0.5–2 μM) inhibition of reporter activity was observed in SYO-1, HS-SY-II (Figure 4a) and CME-1 (Supplementary Figure S3a) cells. Furthermore, increased reporter activity after co-expression of mutant ΔN131 β-catenin was diminished in treated SYO-1 cells (Figure 4b), indicating specific suppression of Wnt/β-catenin signaling in the setting of mesenchymal tumor cells. Immunoblotting of AXIN2, CDC25A, c-MYC, DKK1, CyclinD1 and Survivin revealed a dose- and time-dependent downregulation in SYO-1, HS-SY-II and CME-1 cells (Figures 4c–d, Supplementary Figure S3b and data not shown), with no alterations in the nuclear fractions of β-catenin observed (data not shown).

PKF115–584, CGP049090 and PKF118–310 inhibit cell proliferation by inducing apoptosis and decreasing mitotic activity in synovial sarcoma cell lines

Performing flow cytometric analysis, poly-adenosine diphosphate (ADP)-ribose polymerase (PARP; Asp214) cleavage was used as a marker for apoptosis and phospho-histone H3 (Ser10) was employed as a marker for mitosis. After treatment with PKF115-584, CGP049090 and PKF118-310 (0.1 μM), SYO-1 and CME-1 cells showed significantly increased rates of apoptosis, accompanied by decreased mitotic fractions (Figure 5a, Table 2 and Supplementary

Figure S3c). Consistently, immunoblot analyses of treated synovial sarcoma cells demonstrated an induction of caspase-3 cleavage in a dose-dependent manner (Figure 5b and Supplementary Figure S3d). Similar results were observed in HS-SY-II cells (data not shown).

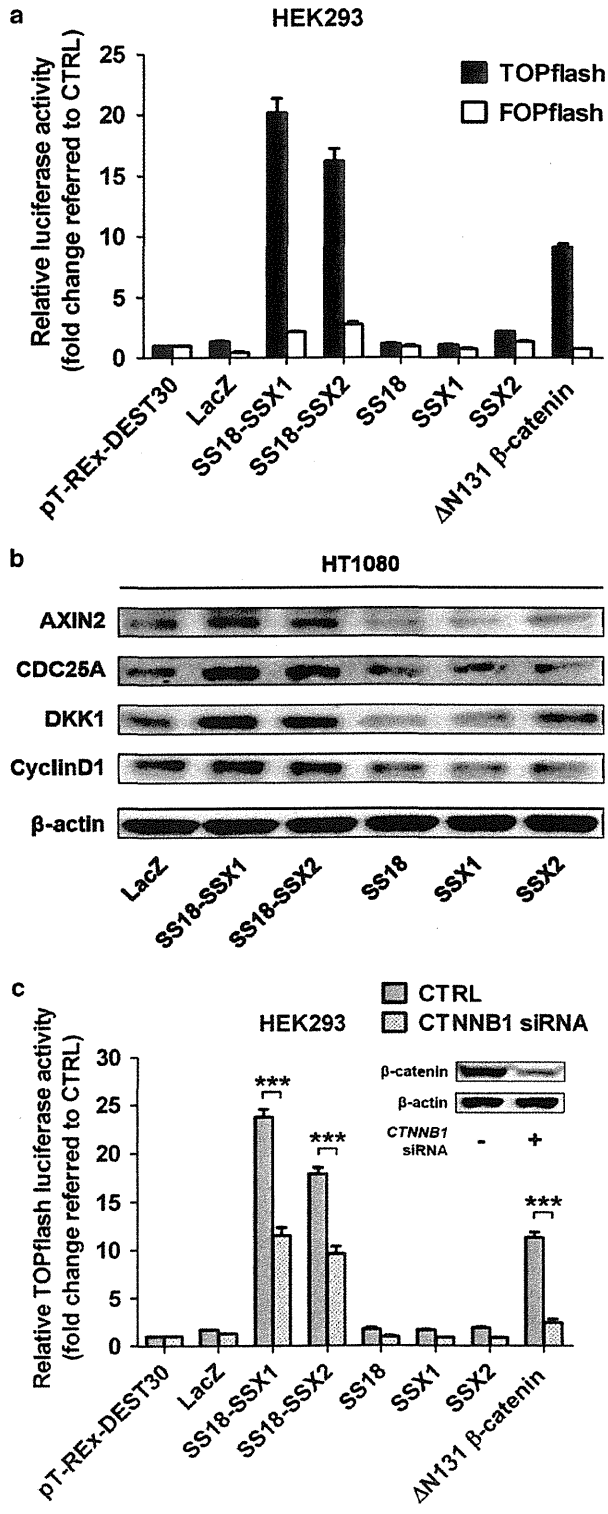

Knockdown of *CTNNB1* and *SS18-SSX2* affect cell viability and Wnt target expression in synovial sarcoma cell lines

To document the functional role of β-catenin by an independent non-pharmacological approach, synovial sarcoma cell lines (SYO-1, HS-SY-II and CME-1) were transfected with siRNAs directed against human *CTNNB1* (encoding β-catenin). In MTT assays, all analyzed synovial sarcoma cell lines displayed significantly reduced cell viabilities (***$P<0.001$; **$P<0.01$) in comparison with non-targeting control siRNA (Figure 6a and Supplementary Figure S4a). Consistently, siRNA-mediated knockdown of β-catenin leads to reduced Wnt target gene expression, combined with the induction of caspase-3 cleavage (Figure 6b and Supplementary Figure S4b). To inversely prove the contribution of SS18-SSX2 to Tcf/β-catenin-mediated transcriptional activity, synovial sarcoma cells (SYO-1, FUJI, 1273/99 and CME-1) were transfected with a set of published and validated siRNA duplex oligos targeting the SSX2 portion of the chimeric oncoprotein.[31,32] Upon decreased SS18-SSX2 expression, all analyzed cell lines displayed reduced Wnt target expression (Figure 6c), implying that the SS18-SSX2 fusion protein is involved in the regulation of Tcf/β-catenin-mediated transcriptional activity. Consistent with the elevated expression levels of Wnt/β-catenin signaling targets upon *SS18-SSX* transfection (Figure 2b), expression of AXIN2, DKK1 and CyclinD1 was inversely suppressed compared with non-targeting negative control siRNA (Figure 6c).

In vivo efficacy of CGP049090 in a murine xenograft model of synovial sarcoma

To investigate the *in vivo* efficacy of Tcf/β-catenin complex inhibition on tumor growth and progression in a xenograft mouse model of human synovial sarcoma, we selected CGP049090 as previously published small molecule inhibitor with no major toxic side effects observed.[22,33,34] SYO-1 cells were injected subcutaneously into the lower flank of nude mice to initiate tumor formation. When the tumor volume reached around 100 mm^3, tumor-bearing mice were treated daily with 25 mg/kg CGP049090 ($n=6$) or DMSO vehicle ($n=6$) for 14 days. CGP049090 administration resulted in a significant reduction in tumor volume (Figure 7a and Table 3; *$P<0.05$) compared with the DMSO vehicle control group and did not induce any significant effects on body weights (Figure 7b and Table 3). Immunohistochemical analysis of tumor sections revealed that Tcf/β-catenin inhibition was associated with decreased AXIN2 protein levels (Figure 7c). The percentage of phospho-histone H3 (Ser10)- positive mitotic cells was significantly decreased in CGP049090-treated tumors compared with vehicle-treated

Figure 2. Synovial sarcoma-associated SS18-SSX fusion proteins stimulate Tcf/β-catenin-mediated transcriptional activity. (**a**) HEK293 cells were co-transfected with indicated SS18-SSX, SS18 or SSX expression vector, and TOP-/FOPflash luciferase reporter plasmids to study Tcf/β-catenin-mediated transcriptional activity. Luciferase reporter activities were measured 24 h after transfection and normalized to *Renilla* luciferase activities. Co-expression of *SS18-SSX1* and *SS18-SSX2* significantly increased TOPflash reporter activity compared with *SS18*, *SSX1* or *SSX2*, confirming stimulated Tcf/β-catenin activity. Experiments were performed in triplicates; results are expressed as mean ± s.d. (**b**) Elevated Wnt target protein levels of AXIN2, CDC25A, DKK1 and CyclinD1 in HT1080 cells expressing the SS18-SSX fusion proteins. (**c**) Significant reduction of TOPflash reporter activity upon siRNA-mediated knockdown of β-catenin (inset) in HEK293 cells co-transfected with SS18-SSX1 and SS18-SSX2 expression vectors and TOPflash reporter plasmids, indicating requirement of β-catenin for SS18-SSX stimulated reporter activation. Luciferase reporter activities were measured 72 h after siRNA transfection and were normalized to *Renilla* luciferase activities.

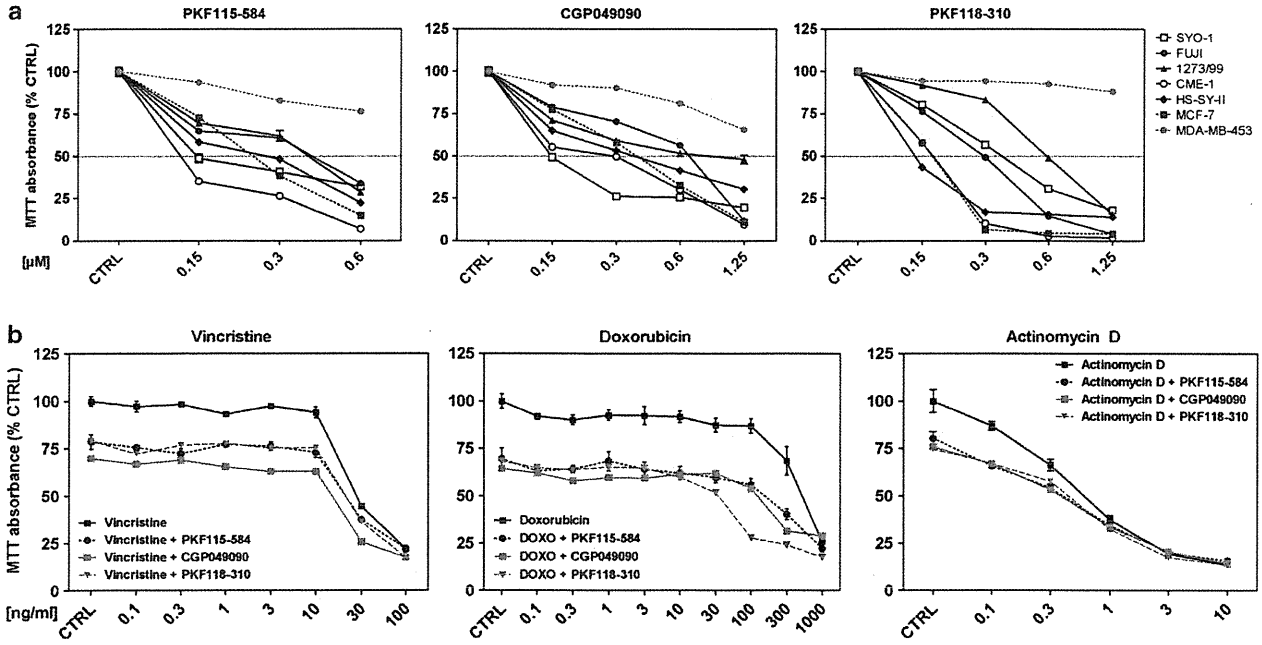

Figure 3. *In vitro* cytotoxic effects of PKF115–584, CGP049090 and PKF118–310 on synovial sarcoma cell lines. (**a**) Cell viability of synovial sarcoma cell lines was inhibited by treatment with increasing concentrations (0.15–1.25 µM) of PKF115–584, CGP049090 and PKF118–310. MCF-7 and MDA-MB-453 breast cancer cells were included as positive and negative controls, respectively. At least three independent experiments were performed (each in quintuplicate), results are expressed as mean ± s.e. (**b**) Combined treatment of SYO-1 cells with conventional chemotherapeutic agents (Vincristine, Doxorubicin and Actinomycin D; 0.1–1000 ng/ml) and small molecular inhibitors of the Tcf/β-catenin protein–protein interaction (0.1-0.2 µM; concentration resulting in 20–30% growth inhibition) resulted in additive effects.

Table 1. IC_{50} values for PKF115–584, CGP049090 and PKF118–310 in synovial sarcoma and breast carcinoma cell lines

Compound	*IC_{50} (µM)*						
	SYO-1	*FUJI*	*1273/99*	*CME-1*	*HS-SY-II*	*MCF-7*	*MDA-MB-453*
PKF115-584	0.18 ± 0.02	0.40 ± 0.03	0.39 ± 0.02	0.25 ± 0.06	0.37 ± 0.09	0.37 ± 0.09	ND
CGP049090	0.19 ± 0.04	0.91 ± 0.21	1.82 ± 0.92	0.41 ± 0.03	0.81 ± 0.11	0.61 ± 0.14	ND
PKF118-310	0.38 ± 0.01	0.30 ± 0.01	0.60 ± 0.02	0.22 ± 0.02	0.17 ± 0.03	0.18 ± 0.01	ND

Effects of small molecule inhibitors PKF115–584, CGP049090 and PKF118–310 on synovial sarcoma and control breast carcinoma cell viability were assessed in MTT assays (72 h). Results are represented as mean ± s.e. of at least three separate experiments performed in quintuplicates (ND, not determined).

controls (Figures 7c and d; $^{***}P<0.001$); as cleaved caspase-3 (Asp175) levels were significantly increased upon CGP049090 treatment (Figures 7c and e; $^{**}P<0.01$).

DISCUSSION

Synovial sarcoma is a highly malignant mesenchymal tumor with a dismal prognosis in patients with advanced metastasized disease. Current therapeutic concepts are mainly based on radical surgery and conventional radiotherapeutic protocols. Synovial sarcoma is characterized by specific oncogenic SS18-SSX fusion proteins, which are of crucial importance in tumor development, as has convincingly been demonstrated in a conditional synovial sarcoma mouse model.[4,35,36] The SS18-SSX fusion proteins act as transcriptional regulators through complex interaction with various partners within chromatin remodeling complexes, thereby dysregulating gene expression.[5–8] As it is particularly challenging to specifically target these chimeric fusion proteins within regulatory active complexes, it might be more suitable to search for specific therapeutic targets among oncogenic pathways, which are activated by the SS18-SSX translocation proteins.

One of the deregulated pathways that has recurrently been identified in cDNA expression microarray analyses of synovial sarcoma is the Wnt/β-catenin signaling pathway.[9–13] However, its oncogenic function and potential role as a specific therapeutic target has only partially been analyzed. In a variety of malignancies, activation of Wnt signaling is due to genetic alterations in central pathway components, including *CTNNB1* and *APC*. In synovial sarcoma, such mutations have been reported in a minor frequency, suggesting a regulatory function of the SS18-SSX chimeric oncoproteins.[19,20,37] We therefore set out to analyze the biological role of canonical Wnt/β-catenin signaling in synovial sarcoma, to decipher its functional dependence on the pathognomonic t(X;18) translocation and to determine whether molecularly targeted interventions with Wnt signals might represent a novel therapeutic option for the treatment of synovial sarcoma.

In accordance with previous studies, we found nuclear accumulation of β-catenin, representing a strong indication of

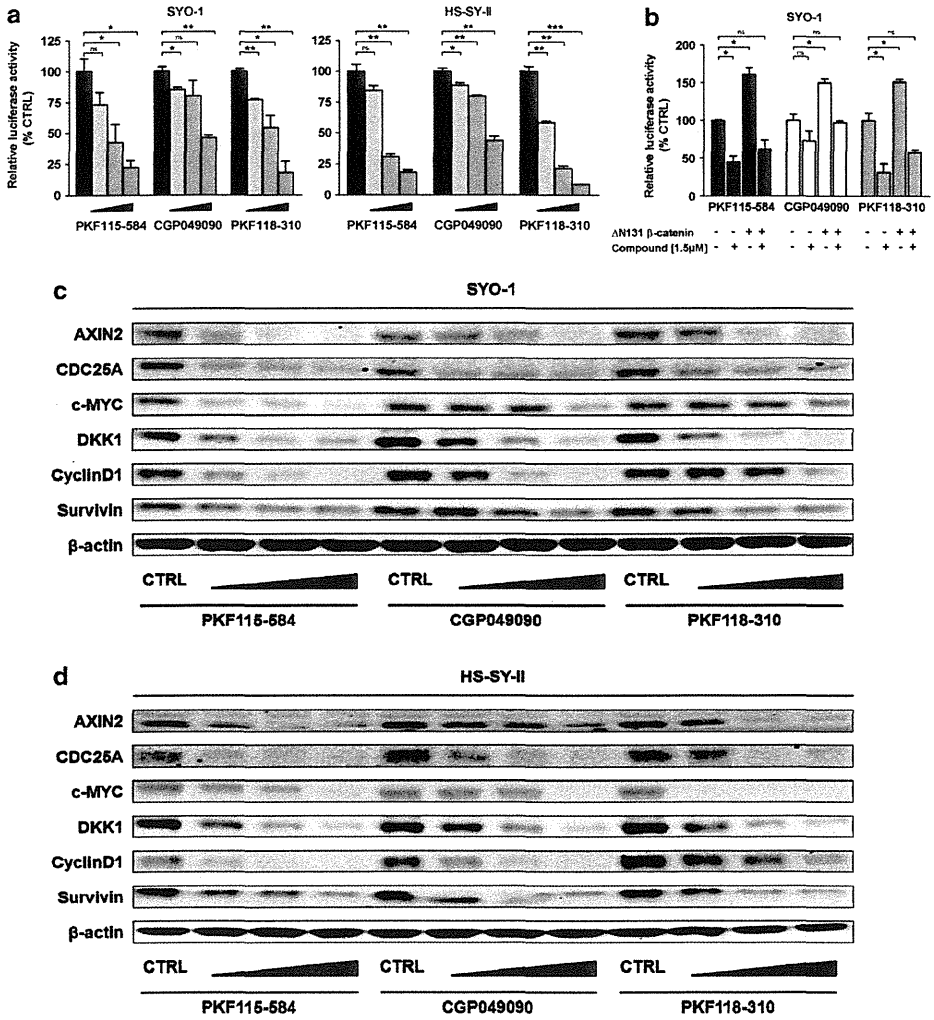

Figure 4. PKF115–584, CGP049090 and PKF118–310 inhibit Tcf/β-catenin interaction and transcriptional activity in synovial sarcoma cell lines. (**a**) SYO-1 and HS-SY-II cells were transfected with the TOPflash luciferase reporter plasmid and treated with increasing concentrations (0.5–2 μM; 24 h) of PKF115–584, CGP049090 and PKF118–310. In response to treatment with all three compounds, significant dose-dependent inhibition of luciferase activity was observed in both cell lines. Experiments were performed in triplicates, results are expressed as mean ± s.d. (**b**) In SYO-1 cells, TOPflash reporter activity was significantly enhanced after co-expression of mutant ΔN131 β-catenin and reversed upon treatment with PKF115–584, CGP049090 and PKF118–310 (1.5 μM). (**c**) Compounds inhibit Tcf/β-catenin-regulated expression of AXIN2, CDC25A, c-MYC, DKK1, CyclinD1 and Survivin in SYO-1 and (**d**) HS-SY-II cells. Synovial sarcoma cells were treated with increasing concentrations of the substances (0.5–2 μM) for 15 h. Changes in target expression were determined by immunoblotting.

activated Wnt/β-catenin signaling to be a frequent feature in synovial sarcoma.[37–39] In tumor-derived synovial sarcoma cell lines, we could additionally show that β-catenin was predominantly present in the non-phosphorylated (Ser33/-37/Thr41 and Ser45), and transcriptionally active form. Consistently, expression of Wnt/β-catenin signaling targets AXIN2, CDC25A, c-MYC, DKK1, CyclinD1 and Survivin was found strongly elevated in four out of five synovial sarcoma cell lines. The expression of these targets was increased in primary tumors with nuclear β-catenin reactivity compared with β-catenin-negative tumors. Accordingly, in 1273/99 synovial sarcoma cells, low nuclear β-catenin levels were associated with minor expression levels of Wnt targets, serving as further evidence for the Wnt-dependent regulation of these targets in synovial sarcoma.

To comprehensively understand the oncogenic mechanisms leading to aberrant activation of Wnt/β-catenin signaling, we explored the molecular dependence of Wnt signals on the pathognomonic SS18-SSX fusion proteins. In response to *SS18-SSX* expression, significantly induced TOPflash reporter luciferase activity was seen in HEK293 cells, demonstrating a pronounced induction of Tcf/β-catenin-mediated transcriptional activity.

As synovial sarcomas are mesenchymal tumors, we chose HT1080 fibrosarcoma cells for further analyses. Upon expression of *SS18-SSX*, HT1080 cells displayed elevated protein levels of AXIN2, CDC25A, DKK1 and CyclinD1. Inversely, in synovial sarcoma cell lines, downregulation of *SS18-SSX2* negatively regulated Wnt signaling activity as indicated by altered target gene expression. Coherently, siRNA-mediated knockdown of β-catenin affected its transcriptional function and the expression of target genes in synovial sarcoma cell lines. Collectively, these observations highlight that the SS18-SSX fusion proteins cooperate to synovial sarcoma tumorigenesis by activation of the Tcf/β-catenin transcription complex. The mechanism of activation and regulation of the Wnt signaling pathway is subject to on-going investigation,

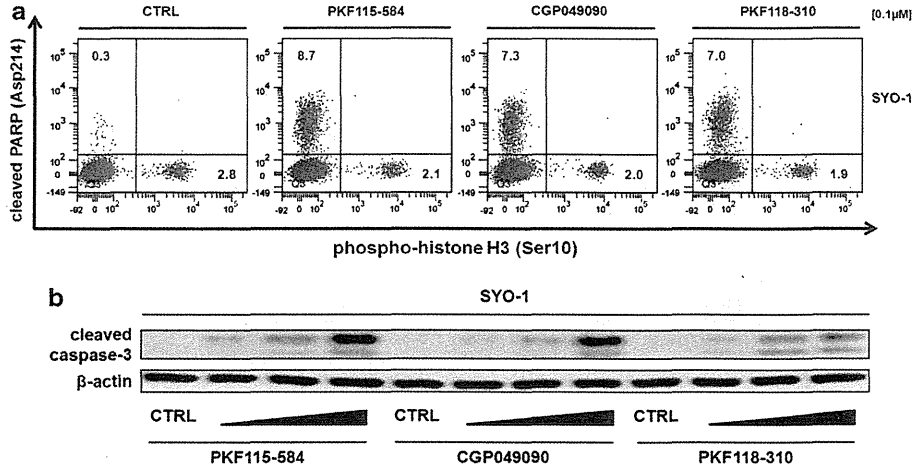

Figure 5. PKF115–584, CGP049090 and PKF118–310 induce apoptosis and impair proliferation of SYO-1 synovial sarcoma cells. (**a**) Representative results of flow cytometric analysis of cleaved PARP (Asp214) and phospho-histone H3 (Ser10) in treated SYO-1 cells. DMSO was employed as control. Significantly increased rates of apoptosis (cleaved PARP) and decreased mitotic fractions (phospho-histone H3) were detected upon treatment with indicated compounds (0.1 μM; 24 h). (**b**) Increasing concentrations of PKF115-584, CGP049090 and PKF118–310 resulted in induced caspase-3 cleavage in SYO-1 cells.

Table 2. Results of flow cytometric analysis in synovial sarcoma cell lines

Cell line	*Compound*	*p-histone H3 (Ser10) (fold change)*	*Cleaved PARP (Asp214) (fold change)*
SYO-1	PKF115-584	0.75 ± 0.05	33.8 ± 1.41
	CGP049090	0.71 ± 0.03	29.0 ± 0.28
	PKF118-310	0.68 ± 0.03	27.4 ± 0.85
CME-1	PKF115-584	0.69 ± 0.02	7.25 ± 0.79
	CGP049090	0.73 ± 0.03	5.25 ± 0.16
	PKF118-310	0.75 ± 0.02	10.75 ± 0.79

Fold changes of apoptotic (cleaved PARP; Asp214) and mitotic (phospho-histone H3; Ser10) fractions upon treatment with PKF115–584, CGP049090 and PKF118–310 (0.1 μM; 24 h) referred to control cells (mean ± s.d.).

with the SS18-SSX oncoproteins being involved in Polycomb and SWI/SNF chromatin remodeling complexes and multiprotein complexes associated with ATF2 and TLE1.[40] Recently, it was shown that the oncogenic SS18-SSX fusion protein incorporates into the SWI/SNF (BAF) chromatin-remodeling complex displacing wild-type SS18, thereby leading to an induction of Sox2 expression and subsequent cellular proliferation.[41] Interestingly, Sox2 has been identified to act as a transcriptional partner of β-catenin, synergizing in the transcriptional induction of the Wnt target *CyclinD1* in breast cancer cells.[42] Sox2 is uniformly expressed and activated in synovial sarcoma.[43]

Previous experiments in NIH3T3 cells demonstrated that exogenous expression of *SS18-SSX2* stimulates the nuclear recruitment of β-catenin, forming a transcriptionally active complex (containing SS18-SSX2 and β-catenin) to potentiate Tcf/β-catenin-mediated reporter activity in a p300-dependent manner. However, expression of the Wnt signaling targets CyclinD1 and c-MYC was not found to be enhanced in these studies, which leads the authors to delineate a non-canonical Wnt context in synovial sarcoma.[31]

Small molecule inhibitors of the Tcf/β-catenin protein complex[22–24] have been found to possess antitumor activities against the central key mediator of canonical Wnt/β-catenin signaling in solid tumors as hepatocellular carcinoma[34] and hematopoietic malignancies as chronic lymphocytic leukemia.[33] Being the first to apply these substances in a malignant mesenchymal tumor, we here show that these compounds effectively counteract Wnt/β-catenin signal transduction in five human synovial sarcoma cell lines *in vitro*, including both major SS18-SSX translocation subtypes. Cellular proliferation and viability were significantly reduced in a dose- and time-dependent manner, associated with decreased TOPflash luciferase reporter activities and Wnt/β-catenin target expression. Combined treatments with conventional chemotherapeutic agents (Vincristine, Doxorubicin and Actinomycin D) resulted in additive effects. Treatment with PKF115–584, CGP049090 and PKF118–310 reduced the mitotic fraction of synovial sarcoma cells and induced apoptosis. Consistent with these *in vitro* results, administration of CGP049090 significantly inhibited tumor growth in SYO-1 synovial sarcoma xenografts *in vivo*, accompanied with an induction of apoptosis and down-regulation of AXIN2 expression. In summary, our data indicate that inhibition of Wnt/β-catenin signaling by treatment with small molecule inhibitors of the Tcf/β-catenin protein complex possesses antitumor potentials in synovial sarcoma xenografts.

In conclusion, the results of the current study imply that the expression of regulatory oncogenes promoting cell cycle progression and cellular proliferation is transcriptionally controlled by the Wnt/β-catenin signaling pathway in a SS18-SSX-dependent manner. Disruption of the Tcf/β-catenin protein complex via small molecule inhibitors may provide an effective therapeutic approach for the treatment of synovial sarcoma. The present preclinical testing of novel molecularly targeted strategies employing Tcf/β-catenin complex inhibitors shows potent effects *in vitro* and *in vivo*, qualifying the Wnt/β-catenin signaling pathway as a specific therapeutic target in synovial sarcoma.

MATERIALS AND METHODS

Patients, tumor samples and cell lines

The study included primary tumor tissues from 30 synovial sarcoma patients (11 women, 19 men; median age at diagnosis was 43 years, range 7–91 years). Clinicopathologic characteristics are summarized in Supplementary Table S1. Histologically, 22 tumors belong to the monophasic subtype, and 8 tumors were classified as biphasic. Median tumor size was 6 cm (range 0.4–19.5 cm). In all cases, fluorescence *in situ* hybridization (FISH) or PCR analysis confirmed the diagnosis of synovial

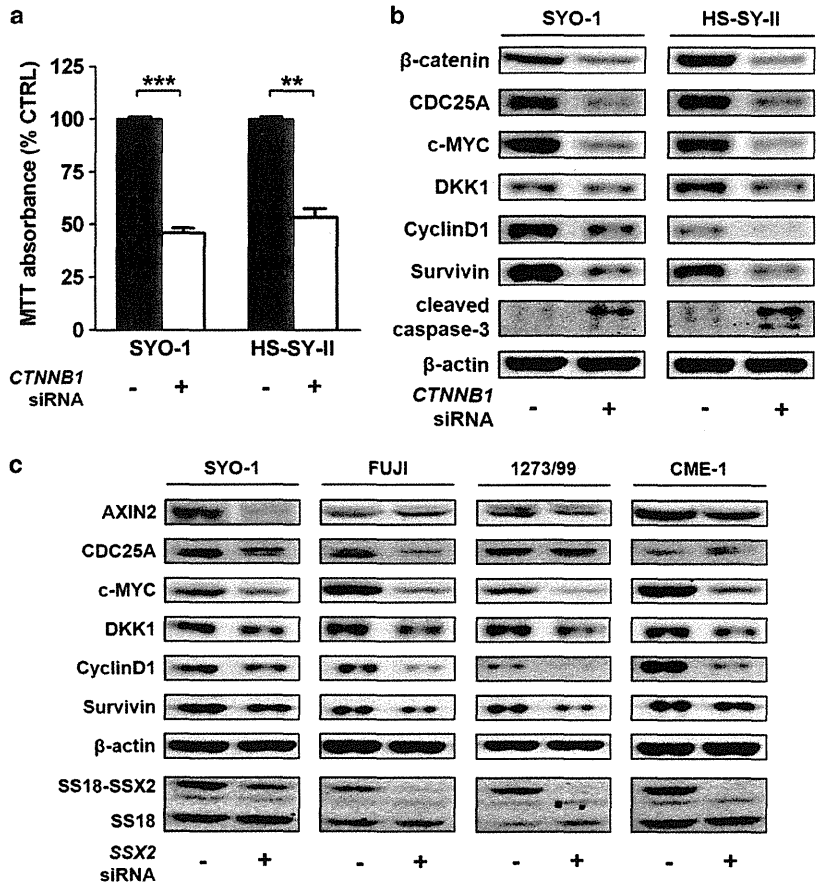

Figure 6. Effects of siRNA-mediated knockdown of β-catenin and SS18-SSX2 on cell viability and Tcf/β-catenin transcriptional activity. (**a**) Significant reduction of cell viability (MTT assay) upon siRNA-mediated knockdown of β-catenin (encoded by *CTNNB1*) in SYO-1 and HS-SY-II synovial sarcoma cells (***$P<0.001$; **$P<0.01$). Experiments were performed in quintuplicates and results of a representative experiment are expressed as mean ± s.d. (**b**) Immunoblotting analyses demonstrate a significant induction of caspase-3 cleavage (Asp175) and a decrease in Wnt/β-catenin signaling target expression following *CTNNB1* or (**c**) *SS18-SSX2*-specific siRNA transfection in four different synovial sarcoma cell lines. Efficient siRNA-mediated *SS18-SSX2* knockdown was confirmed with an antibody targeting the N terminus of the SS18 protein.

sarcoma, revealing the pathognomonic t(X;18) translocation as described previously.[44] Approval of the study by the Ethical Committee of the University of Bonn Medical Center was obtained. The human monophasic synovial sarcoma cell lines HS-SY-II (expressing *SS18-SSX1*), FUJI, 1273/99 and CME-1 and the biphasic SYO-1 cells (all expressing *SS18-SSX2*) were cultured as described previously.[45–47] Presence of the pathognomonic SS18-SSX translocation was confirmed by reverse transcriptional PCR (RT–PCR) using specific primers for the translocation subtypes. The human fibrosarcoma cell line HT1080, human embryonic kidney cells HEK293 and the breast carcinoma cell lines MCF-7 and MDA-MB-453 were obtained from the American Type Culture Collection (ATCC, Manassas, VA, USA). All monolayer cell cultures were grown under standard incubation condition (37 °C, humidified atmosphere, 5% CO_2) and maintained in DMEM (HS-SY-II, SYO-1, HT1080, HEK293, MCF-7 and MDA-MB-453), RPMI 1640 (FUJI and CME-1) or F-12 (1273/99) media, supplemented with 10–15% fetal bovine serum (FBS; Life Technologies, Carlsbad, CA, USA). To study the effects of PKF115–584, CGP049090 and PKF118–310 treatment on Tcf/β-catenin-mediated Wnt signaling, synovial sarcoma cells were grown in six-well plates (medium supplemented with 2% FBS) before treatment with increasing concentrations of the compounds (0–2 μM). Cell lysis, protein extraction and immunoblotting were performed 15 h after treatment as described previously.[48]

Compounds

Small molecule inhibitors of the Tcf/β-catenin protein complex (PKF115–584, CGP049090 and PKF118–310) were provided by Novartis Pharma AG (Basel, Switzerland) and dissolved in dimethyl sulfoxide (DMSO; Sigma-Aldrich, St Louis, MO, USA). The final DMSO concentration did not exceed 0.1% (v/v) for all *in vitro* and *in vivo* applications. Vincristine, Doxorubicin and Actinomycin D were purchased from Sigma-Aldrich.

SS18-SSX fusion protein overexpression in HT1080 cells

The generation of expression plasmids for *SS18-SSX1*, *SS18-SSX2*, *SS18*, *SSX1* and *SSX2* was described previously.[49] HT1080 cells were grown in six-well plates and transfected with 2.5 μg of plasmid DNA using Lipofectamine 2000 (Life Technologies) according to the manufacturer's instructions. Expression was confirmed 24 h after transfection by immunoblotting and RT–PCR. As a control, HT1080 cells were transfected with the pT-REx/GW-30/*lacZ* plasmid (Life Technologies) expressing β-galactosidase.

Luciferase reporter assay

To assess Tcf/β-catenin-mediated transcriptional activity, TOP-/FOPflash luciferase reporter gene assays were performed using the Dual-Luciferase Reporter Assay System (Promega, Madison, WI, USA) according to the manufacturer's instructions.[50] HEK293 cells were transiently transfected with *Firefly* TOPflash or the control FOPflash plasmid DNA (Merck Millipore, Darmstadt, Germany) containing wild-type or mutant Tcf DNA-binding sites, respectively. For extrinsic activation of Wnt/β-catenin signaling, cells were co-transfected with the mutant ΔN131 β-catenin plasmid. The amount of plasmid DNA in each transfection was kept constant by addition of the empty pcDNA3.1 plasmid. After incubation for 24 h, cells were lysed and luciferase activity was measured in triplicates as described previously.[51] *Firefly* luciferase activity was normalized to the co-transfected *Renilla* pRL-TK control plasmid (Promega) to account for

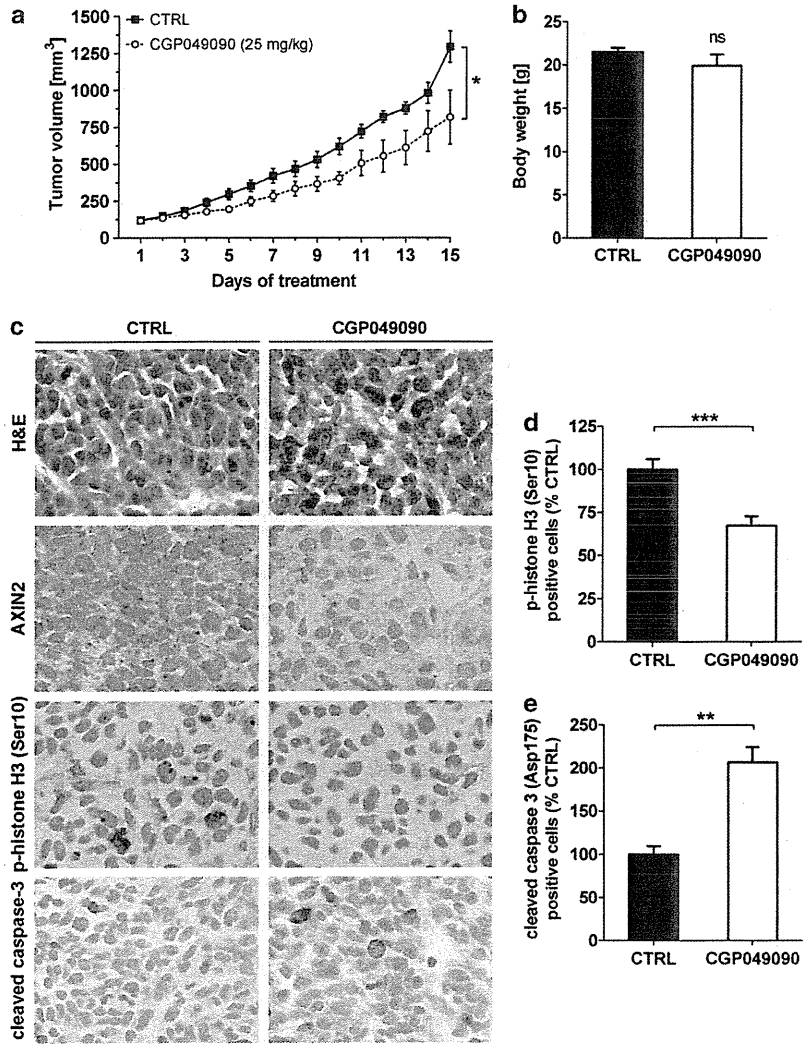

Figure 7. CGP049090 inhibits synovial sarcoma xenograft growth *in vivo*. Mice bearing SYO-1 tumors were randomized ($n = 6$ per group) and treated daily with CGP049090 (25 mg/kg) or DMSO vehicle control for 14 days. (**a**) Mean tumor volume ± s.e. at given time points and (**b**) mean of body weight during killing for SYO-1 xenografts are shown. Mice treated with CGP049090 exhibited significantly reduced tumor volumes (*$P < 0.05$). (**c**) Xenograft tumor tissues from vehicle-treated (left) and CGP049090-treated (right) mice were subjected to immunohistochemical analyses of AXIN2, phospho-histone H3 (Ser10) and cleaved caspase-3 (Asp175) (original magnification, × 40). (**d**) Phospho-histone H3 (Ser10)-positive mitotic cells and (**e**) cleaved caspase-3 (Asp175)-positive apoptotic cells were counted from randomly selected areas and are indicated as mean ± s.e. Tumor growth reduction was associated with decreased levels of phospho-histone H3 (Ser10) (***$P < 0.001$) and an induction of cleaved caspase-3 (Asp175)-positive apoptotic cell fraction (**$P < 0.01$).

Table 3. Effects of CGP049090 treatment on tumor volume and body weight of SYO-1 xenografts

Treatment	*Tumor volume (mm^3)*		*Body weight (g)*	
	Initial	*Final*	*Initial*	*Final*
CTRL	120.4 ± 5.2	1294.6 ± 97.5	21.9 ± 0.4	21.5 ± 0.5
CGP049090	118.4 ± 6.3	816.0 ± 166.9*	19.7 ± 0.6	19.3 ± 1.3^{NS}

Mice were treated daily with CGP049090 (25 mg/kg) or DMSO as control for 14 days. Results are represented as mean ± s.e. Asterisks indicate significant difference (*$P < 0.05$; NS, not significant; Student's *t*-test).

potential differences in transfection efficiency. SYO-1, CME-1 and HS-SY-II cells were transfected with TOP-/FOPflash plasmid DNA to determine the ability of PKF115–584, CGP049090 and PKF118–310 to disrupt Tcf/β-catenin complex formation and associated transcriptional activity. After 6 h, medium containing transfection reagent was replaced with new culture medium supplemented with indicated concentrations (0.5–2 μM; 2% FBS) of each compound for additional 18 h. Luciferase reporter activity was assayed as described above.

Cell viability assay (MTT)

Cell viability was measured using the MTT cell proliferation kit (Roche, Basel, Switzerland) according to the manufacturer's instructions. SYO-1 (5×10^3), FUJI (7.5×10^3), 1273/99 (7.5×10^3), CME-1 (5×10^3), HS-SY-II (7.5×10^3), MCF-7 (7.5×10^3), and MDA-MB-453 (7.5×10^3) cells were seeded in 96-well plates (100 μl of medium supplemented with 2% FBS) and exposed to increasing concentrations of PKF115–584, CGP049090 and PKF118–310 (0.15–1.25 μM) for 72 h. An appropriate DMSO control was included. For combined treatment with chemotherapeutic agents, SYO-1 cells were incubated with increasing concentrations of Vincristine (0.1–100 ng/ml), Doxorubicin (0.1–1000 ng/ml) and Actinomycin D (0.1–10 ng/ml), alone or in combination with PKF115-584, CGP049090 or PKF118–310 (0.1–0.2 μM; concentration resulting in 20–30% growth inhibition). Synergy

was evaluated using the fractional product method.[52] Differences of >10% between the observed and predicted effect were considered to signify synergistic activity between the chemotherapeutic agent and the small molecule inhibitors of the Tcf/β-catenin protein complex, a difference <10% was defined as additive.

RNA interference

Small interference RNA (siRNA) specific for human *CTNNB1* (Stealth Select RNAi siRNA set of 3: HSS102461, HSS102462, HSS102460) and non-targeting negative control siRNA (BLOCK-iT Alexa Fluor Red Fluorescent Control) were purchased from Life Technologies. To target the *SSX2* portion of *SS18-SSX2*, a set of published and validated duplex oligos was employed (sense: 5′-AAC CAA CUA CCU CUG AGA AGA-3′; antisense: 5′-UCU UCU CAG AGG UAG UUG GUU-3′ and sense: 5′-CAA GAA GCC AGC AGA GGA ATT-3′; antisense: 5′-UUC CUC UGC UGG CUU CUU GTT-3′).[31,32] SYO-1, CME-1 and HS-SY-II cells were cultured in 25 cm^2 cell culture flasks (medium supplemented with 10% FBS) and transfected with indicated siRNA (75 pmol; cell density of 50%) using Lipofectamine RNAiMAX (Life Technologies). After incubation for 24 h, siRNA-transfected cells were trypsinized and re-seeded for MTT assays as described above. Knockdown efficiency was documented by immunoblotting.

Immunoblot analysis

Following primary antibodies were used according to the manufacturer's instructions: cleaved caspase-3 (Asp175), CyclinD1, Survivin, β-catenin, and phospho(Ser33/37/Thr41)-β-catenin, phospho(Thr41/Ser45)-β-catenin, phospho(Ser552)-β-catenin, phospho(Ser675)-β-catenin (all obtained from Cell Signaling Technology, Danvers, MA, USA); AXIN2, CDC25A, c-MYC, DKK1 and GAPDH (all obtained from Abcam, Cambridge, UK); SS18 and LaminB1 (Santa Cruz Biotechnology, Dallas, TX, USA); β-actin (Sigma-Aldrich). The SS18-SSX fusion protein was detected with an antibody targeting the N terminus of SS18. Secondary antibody labeling (Bio-Rad Laboratories, Hercules, CA, USA) as well as immunoblot development was performed using the enhanced chemiluminescence detection kit (Amersham Biosciences, Little Chalfont, UK) as described before. Subcellular fractionation was performed using the NE-PER Nuclear and Cytoplasmic Extraction Reagents kit (Pierce Biotechnology, Rockford, IL, USA) according to the manufacturer's instructions.

Flow cytometry

The effect of PKF115-584, CGP049090 and PKF118-310 on synovial sarcoma apoptosis and cell proliferation was assessed by flow cytometric analysis. Briefly, SYO-1 and CME-1 cells were grown in 75 cm^2 cell culture flasks (medium supplemented with 2% FBS) and treated with 0.1 μM of the compounds for 24 h. Cells were fixed in 2% paraformaldehyde for 10 min on ice, washed in PBS, collected by centrifugation and incubated in ice-cold PBS with 0.25% Triton X-100 for 5 min on ice. After an additional washing step, cells were resuspended in 100 μl PBS/0.5% BSA containing following antibodies: cleaved Poly-(ADP-ribose)-polymerase (PARP) (Asp214) (BD Biosciences, San Jose, CA, USA; phycoerythrin-labeled) and phospho-histone H3 (Ser10) (Cell Signaling Technology; Alexa Fluor 647-labeled) followed by incubation for 30 min at room temperature. Fluorescence intensity was measured using a LSRII analytical flow cytometer (BD Biosciences), and cytometric data were analyzed using the FlowJo (Tree Star, Ashland, OR, USA) software. Each experiment was carried out at least in duplicates.

In vivo efficacy of CGP049090 in synovial sarcoma xenograft studies

SYO-1 cells (5×10^6) were injected subcutaneously into the lower flank region of male BALB/c-nude mice (Charles River Laboratories, Wilmington, MA, USA; 5 weeks old). Tumor growth was monitored daily, and tumor volume was calculated according to the formula: TV = length (mm) × width (mm) × height (mm) × π/6. Treatment was initiated once the tumor volume reached ~100 mm^3. To evaluate the *in vivo* antitumor efficacy of CGP049090, tumor-bearing mice were randomly assigned into two treatment groups and received 25 mg/kg CGP049090 ($n = 6$) or DMSO (vehicle control; $n = 6$) every other day via intraperitoneal (i.p.) administration. After 15 days of treatment, mice were killed, with tumor volume, body weights and general physical status recorded. Tumor tissues were explanted, followed by immunohistochemical and histopathological examination as described above. All studies were performed in accordance with the standards of the National and European Union guidelines, and permission was obtained from the local authorities.

Statistical analysis

The immunohistochemical results were statistically analyzed using Fisher's exact test. Results of MTT assays and flow cytometric analyses are represented as mean ± s.d. or s.e. from *n* independent experiments. Two-group comparisons were analyzed by unpaired Student's *t*-test. Statistical differences were considered significant at $P < 0.05$. Statistical probability is indicated as follows: $^*P < 0.05$; $^{**}P < 0.01$ and $^{***}P < 0.001$. The compound concentration, which is required for 50% growth inhibition (IC_{50} value), was calculated by non-linear regression analysis using the GraphPad Prism (GraphPad Software, La Jolla, CA, USA).

CONFLICT OF INTEREST

E Wardelmann has received honoraria from speakers' bureau of Novartis Oncology, MSD and Eisai, and is a scientific consultant/advisory board member of Novartis Oncology and MSD. The remaining authors declare no conflict of interest.

ACKNOWLEDGEMENTS

PKF115-584, CGP049090 and PKF118-310 were generously provided by A Wood (Novartis Pharma AG, Basel, Switzerland). This study was supported by Wilhelm Sander-Stiftung, Dr Eberhard und Hilde Rüdiger Stiftung, Deutsche Krebshilfe (KoSar sarcoma competence network), BONFOR (Medical Faculty, University Hospital Bonn, Bonn) and Fortune program (Medical Faculty, University of Cologne, Cologne).

REFERENCES

1 Weiss SW, Goldblum JR, Folpe AL. Enzinger and Weiss's Soft Tissue Tumors Elsevier Health Sciences 2007.
2 Turc-Carel C, Dal Cin P, Limon J, Li F, Sandberg AA. Translocation X;18 in synovial sarcoma. *Cancer Genet Cytogenet* 1986; **23**: 93.
3 Clark J, Rocques PJ, Crew AJ, Gill S, Shipley J, Chan AM *et al.* Identification of novel genes, SYT and SSX, involved in the t(X;18)(p11.2;q11.2) translocation found in human synovial sarcoma. *Nat Genet* 1994; **7**: 502–508.
4 Haldar M, Randall RL, Capecchi MR. Synovial sarcoma: from genetics to genetic-based animal modeling. *Clin Orthop Relat Res* 2008; **466**: 2156–2167.
5 Soulez M, Saurin AJ, Freemont PS, Knight JC. SSX and the synovial-sarcoma-specific chimaeric protein SYT-SSX co-localize with the human Polycomb group complex. *Oncogene* 1999; **18**: 2739–2746.
6 Nagai M, Tanaka S, Tsuda M, Endo S, Kato H, Sonobe H *et al.* Analysis of transforming activity of human synovial sarcoma-associated chimeric protein SYT-SSX1 bound to chromatin remodeling factor hBRM/hSNF2 alpha. *Proc Natl Acad Sci USA* 2001; **98**: 3843–3848.
7 de Bruijn DR, Allander SV, van Dijk AH, Willemse MP, Thijssen J, van Groningen JJ *et al.* The synovial-sarcoma-associated SS18-SSX2 fusion protein induces epigenetic gene (de)regulation. *Cancer Res* 2006; **66**: 9474–9482.
8 Garcia CB, Shaffer CM, Eid JE. Genome-wide recruitment to Polycomb-modified chromatin and activity regulation of the synovial sarcoma oncogene SYT-SSX2. *BMC Genomics* 2012; **13**: 189.
9 Nielsen TO, West RB, Linn SC, Alter O, Knowling MA, O'Connell JX *et al.* Molecular characterisation of soft tissue tumours: a gene expression study. *Lancet* 2002; **359**: 1301–1307.
10 Nagayama S, Katagiri T, Tsunoda T, Hosaka T, Nakashima Y, Araki N *et al.* Genome-wide analysis of gene expression in synovial sarcomas using a cDNA microarray. *Cancer Res* 2002; **62**: 5859–5866.
11 Segal NH, Pavlidis P, Antonescu CR, Maki RG, Noble WS, DeSantis D *et al.* Classification and subtype prediction of adult soft tissue sarcoma by functional genomics. *Am J Pathol* 2003; **163**: 691–700.
12 Baird K, Davis S, Antonescu CR, Harper UL, Walker RL, Chen Y *et al.* Gene expression profiling of human sarcomas: insights into sarcoma biology. *Cancer Res* 2005; **65**: 9226–9235.
13 Francis P, Namlos HM, Muller C, Eden P, Fernebro J, Berner JM *et al.* Diagnostic and prognostic gene expression signatures in 177 soft tissue sarcomas: hypoxia-induced transcription profile signifies metastatic potential. *BMC Genomics* 2007; **8**: 73.
14 Barker N, Clevers H. Mining the Wnt pathway for cancer therapeutics. *Nat Rev Drug Discov* 2006; **5**: 997–1014.
15 Clevers H, Nusse R. Wnt/β-Catenin Signaling and Disease. *Cell* 2012; **149**: 1192–1205.
16 Klaus A, Birchmeier W. Wnt signalling and its impact on development and cancer. *Nat Rev Cancer* 2008; **8**: 387–398.

17 Vijayakumar S, Liu G, Rus IA, Yao S, Chen Y, Akiri G *et al.* High-frequency canonical Wnt activation in multiple sarcoma subtypes drives proliferation through a TCF/beta-catenin target gene, CDC25A. *Cancer Cell* 2011; **19**: 601–612.
18 Anastas JN, Moon RT. WNT signalling pathways as therapeutic targets in cancer. *Nat Rev Cancer* 2013; **13**: 11–26.
19 Saito T, Oda Y, Sakamoto A, Tamiya S, Kinukawa N, Hayashi K *et al.* Prognostic value of the preserved expression of the E-cadherin and catenin families of adhesion molecules and of beta-catenin mutations in synovial sarcoma. *J Pathol* 2000; **192**: 342–350.
20 Saito T, Oda Y, Sakamoto A, Kawaguchi K, Tanaka K, Matsuda S *et al.* APC mutations in synovial sarcoma. *J Pathol* 2002; **196**: 445–449.
21 Barretina J, Taylor BS, Banerji S, Ramos AH, Lagos-Quintana M, Decarolis PL *et al.* Subtype-specific genomic alterations define new targets for soft-tissue sarcoma therapy. *Nat Genet* 2010; **42**: 715–721.
22 Lepourcelet M, Chen YN, France DS, Wang H, Crews P, Petersen F *et al.* Small-molecule antagonists of the oncogenic Tcf/beta-catenin protein complex. *Cancer Cell* 2004; **5**: 91–102.
23 Trosset JY, Dalvit C, Knapp S, Fasolini M, Veronesi M, Mantegani S *et al.* Inhibition of protein-protein interactions: the discovery of druglike beta-catenin inhibitors by combining virtual and biophysical screening. *Proteins* 2006; **64**: 60–67.
24 Zhang M, Catrow JL, Ji H. High-Throughput Selectivity Assays for Small-Molecule Inhibitors of β-Catenin/T-Cell Factor Protein–Protein Interactions. *ACS Med Chem Lett* 2013; **4**: 306–311.
25 Cheng GZ, Chan J, Wang Q, Zhang W, Sun CD, Wang LH. Twist transcriptionally up-regulates AKT2 in breast cancer cells leading to increased migration, invasion, and resistance to paclitaxel. *Cancer Res* 2007; **67**: 1979–1987.
26 Kim SY, Dunn IF, Firestein R, Gupta P, Wardwell L, Repich K *et al.* CK1epsilon is required for breast cancers dependent on beta-catenin activity. *PLoS One* 2010; **5**: e8979.
27 Liu C, Li Y, Semenov M, Han C, Baeg GH, Tan Y *et al.* Control of beta-catenin phosphorylation/degradation by a dual-kinase mechanism. *Cell* 2002; **108**: 837–847.
28 Taurin S, Sandbo N, Qin Y, Browning D, Dulin NO. Phosphorylation of beta-catenin by cyclic AMP-dependent protein kinase. *J Biol Chem* 2006; **281**: 9971–9976.
29 Provost E, McCabe A, Stern J, Lizardi I, D'Aquila TG, Rimm DL. Functional correlates of mutation of the Asp32 and Gly34 residues of beta-catenin. *Oncogene* 2005; **24**: 2667–2676.
30 Romagnolo B, Berrebi D, Saadi-Keddoucci S, Porteu A, Pichard AL, Peuchmaur M *et al.* Intestinal dysplasia and adenoma in transgenic mice after overexpression of an activated beta-catenin. *Cancer Res* 1999; **59**: 3875–3879.
31 Pretto D, Barco R, Rivera J, Neel N, Gustavson MD, Eid JE. The synovial sarcoma translocation protein SYT-SSX2 recruits beta-catenin to the nucleus and associates with it in an active complex. *Oncogene* 2006; **25**: 3661–3669.
32 Lubieniecka JM, de Bruijn DR, Su L, van Dijk AH, Subramanian S, van de Rijn M *et al.* Histone deacetylase inhibitors reverse SS18-SSX-mediated polycomb silencing of the tumor suppressor early growth response 1 in synovial sarcoma. *Cancer Res* 2008; **68**: 4303–4310.
33 Gandhirajan RK, Staib PA, Minke K, Gehrke I, Plickert G, Schlosser A *et al.* Small molecule inhibitors of Wnt/beta-catenin/lef-1 signaling induces apoptosis in chronic lymphocytic leukemia cells *in vitro* and *in vivo*. *Neoplasia* 2010; **12**: 326–335.
34 Wei W, Chua MS, Grepper S, So S. Small molecule antagonists of Tcf4/beta-catenin complex inhibit the growth of HCC cells *in vitro* and *in vivo*. *Int J Cancer* 2010; **126**: 2426–2436.
35 Haldar M, Hancock JD, Coffin CM, Lessnick SL, Capecchi MR. A conditional mouse model of synovial sarcoma: insights into a myogenic origin. *Cancer Cell* 2007; **11**: 375–388.
36 Haldar M, Hedberg ML, Hockin MF, Capecchi MR. A CreER-based random induction strategy for modeling translocation-associated sarcomas in mice. *Cancer Res* 2009; **69**: 3657–3664.
37 Ng TL, Gown AM, Barry TS, Cheang MC, Chan AK, Turbin DA *et al.* Nuclear beta-catenin in mesenchymal tumors. *Mod Pathol* 2005; **18**: 68–74.
38 Hasegawa T, Yokoyama R, Matsuno Y, Shimoda T, Hirohashi S. Prognostic significance of histologic grade and nuclear expression of beta-catenin in synovial sarcoma. *Hum Pathol* 2001; **32**: 257–263.
39 Sato H, Hasegawa T, Kanai Y, Tsutsumi Y, Osamura Y, Abe Y *et al.* Expression of cadherins and their undercoat proteins (alpha-, beta-, and gamma-catenins and p120) and accumulation of beta-catenin with no gene mutations in synovial sarcoma. *Virchows Arch* 2001; **438**: 23–30.
40 Su L, Sampaio AV, Jones KB, Pacheco M, Goytain A, Lin S *et al.* Deconstruction of the SS18-SSX fusion oncoprotein complex: insights into disease etiology and therapeutics. *Cancer Cell* 2012; **21**: 333–347.
41 Kadoch C, Crabtree GR. Reversible disruption of mSWI/SNF (BAF) complexes by the SS18-SSX oncogenic fusion in synovial sarcoma. *Cell* 2013; **153**: 71–85.
42 Chen Y, Shi L, Zhang L, Li R, Liang J, Yu W *et al.* The molecular mechanism governing the oncogenic potential of SOX2 in breast cancer. *J Biol Chem* 2008; **283**: 17969–17978.
43 Naka N, Takenaka S, Araki N, Miwa T, Hashimoto N, Yoshioka K *et al.* Synovial sarcoma is a stem cell malignancy. *Stem Cells* 2010; **28**: 1119–1131.
44 Friedrichs N, Kriegl L, Poremba C, Schaefer KL, Gabbert HE, Shimomura A *et al.* Pitfalls in the detection of t(11;22) translocation by fluorescence *in situ* hybridization and RT-PCR: a single-blinded study. *Diagn Mol Pathol* 2006; **15**: 83–89.
45 Nojima T, Wang YS, Abe S, Matsuno T, Yamawaki S, Nagashima K. Morphological and cytogenetic studies of a human synovial sarcoma xenotransplanted into nude mice. *Acta Pathol Jpn* 1990; **40**: 486–493.
46 Sonobe H, Manabe Y, Furihata M, Iwata J, Oka T, Ohtsuki Y *et al.* Establishment and characterization of a new human synovial sarcoma cell line, HS-SY-II. *Lab Invest* 1992; **67**: 498–505.
47 Kawai A, Naito N, Yoshida A, Morimoto Y, Ouchida M, Shimizu K *et al.* Establishment and characterization of a biphasic synovial sarcoma cell line, SYO-1. *Cancer Lett* 2004; **204**: 105–113.
48 Friedrichs N, Küchler J, Endl E, Koch A, Czerwitzki J, Wurst P *et al.* Insulin-like growth factor-1 receptor acts as a growth regulator in synovial sarcoma. *J Pathol* 2008; **216**: 428–439.
49 Michels S, Trautmann M, Sievers E, Kindler D, Huss S, Renner M *et al.* SRC signaling is crucial in the growth of synovial sarcoma cells. *Cancer Res* 2013; **73**: 2518–2528.
50 Korinek V, Barker N, Morin PJ, van Wichen D, de Weger R, Kinzler KW *et al.* Constitutive transcriptional activation by a beta-catenin-Tcf complex in APC −/− colon carcinoma. *Science* 1997; **275**: 1784–1787.
51 Nguyen A, Su L, Campbell B, Poulin NM, Nielsen TO. Synergism of heat shock protein 90 and histone deacetylase inhibitors in synovial sarcoma. *Sarcoma* 2009; **2009**: 794901.
52 Webb JL. *Enzyme and Metabolic Inhibitors*. Academic Press: New York, USA, 1966.

Supplementary Information accompanies this paper on the Oncogene website (http://www.nature.com/onc)

Published OnlineFirst April 15, 2013; DOI: 10.1158/0008-5472.CAN-12-3023

Molecular and Cellular Pathobiology

Cancer Research

SRC Signaling Is Crucial in the Growth of Synovial Sarcoma Cells

Sebastian Michels[1,2], Marcel Trautmann[1], Elisabeth Sievers[1], Dagmar Kindler[1], Sebastian Huss[1], Marcus Renner[4], Nicolaus Friedrichs[1], Jutta Kirfel[2], Susanne Steiner[2], Elmar Endl[3], Peter Wurst[3], Lukas Heukamp[1], Roland Penzel[4], Olle Larsson[5], Akira Kawai[6], Shinya Tanaka[7], Hiroshi Sonobe[8], Peter Schirmacher[4], Gunhild Mechtersheimer[4], Eva Wardelmann[1], Reinhard Büttner[1], and Wolfgang Hartmann[1]

Abstract

Synovial sarcoma is a soft-tissue malignancy characterized by a reciprocal t(X;18) translocation encoding a chimeric transcriptional modifier. Several receptor tyrosine kinases have been found activated in synovial sarcoma; however, no convincing therapeutic concept has emerged from these findings. On the basis of the results of phosphokinase screening arrays, we here investigate the functional and therapeutic relevance of the SRC kinase in synovial sarcoma. Immunohistochemistry of phosphorylated SRC and its regulators CSK and PTP1B (PTPN1) was conducted in 30 synovial sarcomas. Functional aspects of SRC, including dependence of SRC activation on the SS18/SSX fusion proteins, were analyzed *in vitro*. Eventually, synovial sarcoma xenografts were treated with the SRC inhibitor dasatinib *in vivo*. Activated phospho (p)-(Tyr416)-SRC was detected in the majority of tumors; dysregulation of CSK or PTP1B was excluded as the reason for the activation of the kinase. Expression of the SS18/SSX fusion proteins in T-REx-293 cells was associated with increased p-(Tyr416)-SRC levels, linked with an induction of the insulin-like growth factor pathway. Treatment of synovial sarcoma cells with dasatinib led to apoptosis and inhibition of cellular proliferation, associated with reduced phosphorylation of FAK (PTK2), STAT3, IGF-IR, and AKT. Concurrent exposure of cells to dasatinib and chemotherapeutic agents resulted in additive effects. Cellular migration and invasion were dependent on signals transmitted by SRC involving regulation of the Rho GTPases Rac and RhoA. Treatment of nude mice with SYO-1 xenografts with dasatinib significantly inhibited tumor growth *in vivo*. In summary, SRC is of crucial biologic importance and represents a promising therapeutic target in synovial sarcoma. *Cancer Res; 73(8); 2518–28. ©2013 AACR.*

Introduction

Synovial sarcomas account for 5% to 10% of all soft-tissue sarcomas. In the majority, synovial sarcoma arise mainly in adolescents and young adults with predominance in male gender. They are molecularly characterized by a reciprocal t(X; 18) translocation, which juxtaposes the *SS18* gene on chromosome 18 to either the *SSX1*, the *SSX2*, or rarely to the *SSX4* gene on the X chromosome. The SS18/SSX chimeric proteins act as transcriptional coactivators, leading to deregulation of oncogenic pathways (1–3).

Current treatment protocols for synovial sarcoma are based on radical surgery and standardized chemo- and radiotherapy; however, prognosis is still poor in advanced disease (4). Targeted therapeutic approaches, which have significantly improved the clinical course of patients with gastrointestinal stromal tumors (GIST) or dermatofibrosarcoma protuberans, are still lacking for synovial sarcomas (5, 6). Several receptor tyrosine kinases have been shown to be expressed in synovial sarcomas, including the EGF receptor (EGFR; ref. 7) and the insulin-like growth factor-I receptor (IGF-IR; ref. 8), leading to an activation of the PI3K/AKT signaling pathway (9). Non–receptor tyrosine kinases, including members of the SRC family kinases (SFK), are important in tumor cell growth, survival, and motility in different tumor entities, including mesenchymal tumors as osteosarcoma and Ewing sarcoma (10).

The 60-kDa human c-SRC (SRC) tyrosine kinase contains 2 phosphorylation sites regulating its enzymatic activity. Phosphorylation at Tyr527 leads to a reduced activity, whereas

Authors' Affiliations: [1]Department of Pathology, University Hospital Cologne, Cologne; Departments of [2]Pathology and [3]Molecular Medicine, University Hospital Bonn, Bonn; [4]Department of Pathology, University Hospital Heidelberg, Heidelberg, Germany; [5]Department of Oncology-Pathology, Karolinska Hospital, Stockholm, Sweden; [6]Division of Orthopaedic Surgery, National Cancer Center Hospital, Tokyo; [7]Laboratory of Molecular and Cellular Pathology, Hokkaido University Graduate School of Medicine, Sapporo; and [8]Department of Laboratory Medicine, Chungoku Central Hospital, Fukuyama, Hiroshima, Japan

Note: Supplementary data for this article are available at Cancer Research Online (http://cancerres.aacrjournals.org/).

S. Michels and M. Trautmann contributed equally to this work.

Corresponding Author: Wolfgang Hartmann, Department of Pathology, University Hospital Cologne, Kerpener Strasse 62, Cologne D-50937, Germany. Phone 49-221-47898562; Fax: 49-221-4786360; E-mail: wolfgang.hartmann@uk-koeln.de

doi: 10.1158/0008-5472.CAN-12-3023

Published OnlineFirst April 15, 2013; DOI: 10.1158/0008-5472.CAN-12-3023

autophosphorylation at Tyr416 is associated with full kinase activity (11, 12). SRC phosphorylation status is modulated by the c-SRC tyrosine kinase (CSK) and the protein tyrosine phosphatase PTP1B, which modify SRC phosphorylation at Tyr527 (12, 13). CSK has been reported to be critical for SRC deregulation in colon cancer cells (14). Among the PTPs, PTP1B has been shown to be of particular importance, being overexpressed in breast cancer cell lines with elevated SRC activity (15–17). Different receptor tyrosine kinases including the IGF-IR and effectors of the PIK3/AKT, RAS/MAPK, and STAT3 pathways represent important interaction partners of SRC, leading to cellular survival and proliferation. Furthermore, SRC is capable of modulating cell migration and invasion through interaction with integrins, the focal adhesion kinase (FAK), and regulators of the family of Rho-GTPases (18, 19).

The present study was conducted to analyze the functional relevance of SRC signaling in synovial sarcoma biology and to test its potential as a target for innovative therapeutic approaches.

Materials and Methods

Patients, tumor samples, and cell lines

Thirty cases of synovial sarcoma were analyzed comprising 22 monophasic and 8 biphasic tumors. Approval of the study by the Ethical Committee of the University of Bonn Medical Center (Bonn, Germany) was obtained. FISH or PCR analyses were used to confirm the diagnosis of synovial sarcoma revealing a t(X; 18) translocation as described before (20). The synovial sarcoma cell lines CME-1, 1273/99, FUJI, SYO-1 (all carrying a SS18/SSX2 translocation), and HS-SY-II (carrying a SS18/SSX1-translocation) have been described earlier (21–25); presence of the SS18/SSX translocation was confirmed by PCR using primers specific for the translocation subtypes.

Phosphokinase arrays

1273/99 (SS18/SSX2-translocated) and HS-SY-II (SS18/SSX1-translocated) cells were grown for 48 hours in medium supplemented with 10% FBS. Protein extraction and phosphokinase arrays (R&D Systems), comprising spotted antibodies for 46 kinase phosphorylation sites, were conducted as indicated by the manufacturer. Filter development was conducted using the ECL Kit (Amersham) as described before (26). Densitometric analysis was conducted using the ImageJ software (http://rsb.info.nih.gov/ij).

Immunohistochemistry

PTP1B and CSK antibodies were purchased from Abcam, the p-(Ser10)-histone H3 antibody from Merck Millipore, and p-(Tyr416)-SRC, p-(Tyr527)-SRC and cleaved caspase-3 (Asp175) antibodies from Cell Signaling Technologies. Tissue specimens (including xenografts) were fixed in 4% buffered formaldehyde and embedded in paraffin. After antigen retrieval (10 mmol/L sodium citrate buffer, pH 6.0, microwave 600 W, 10 minutes) PTP1B, CSK, p-(Ser10)-histone H3 and cleaved caspase-3 (Asp175) immunohistochemical stainings were conducted on 4-μm sections with an Autostainer (DAKO) or manually [p-(Tyr416)-SRC and p-(Tyr527)-SRC]. For PTP1B and CSK, the antigen–antibody binding was visualized with the avidin–biotin complex (ABC method) using AEC (3-amino-9-ethylcarbazol) or 3,3′-diaminobenzidine (DAB) as chromogen. For p-(Tyr416)-SRC and p-(Tyr527)-SRC stainings, the Catalyzed Signal Amplification System (CSA II; DAKO) was used according to the manufacturer's instructions using DAB as chromogen. Positive and negative control stainings using an appropriate rabbit IgG subtype (DCS) were included. For all proteins, cytoplasmic and membranous immunoreactivity were assessed using a semiquantitative score (negative, weak, moderate, strong) defining the staining intensity in the positive control (invasive ductal breast cancer/intraductal breast cancer) as strong.

SS18/SSX fusion gene overexpression in T-REx-293 cells

T-REx-293 cells were purchased from Invitrogen and cultured in Dulbeccos' Modified Eagles' Media (DMEM) supplemented with 10% FBS, 2 mmol/L L-glutamine, and 5 μg/mL blasticidin. *SS18/SSX1*, *SS18/SSX2*, *SS18*, *SSX1*, and *SSX2* were amplified by PCR using templates expression vectors described before (27, 28). The cDNAs were then cloned into the tetracycline-regulated pTREx DEST30 Gateway expression vector (Invitrogen). Using Lipofectamine 2000 reagent, T-REx-293 cells were transfected with expression vectors for *SS18/SSX1*, *SS18/SSX2*, *SS18*, *SSX1*, and *SSX2*, respectively, and the pT-REx/GW-30/*lacZ* vector (Invitrogen) expressing β-galactosidase was included as control. Forty-eight hours after transfection, T-REx-293 cells were selected in culture medium supplemented with 1 mg/mL geneticin (G418), and drug-resistant colonies were isolated after 6 weeks of selection. To induce gene expression, 1 μg/mL tetracycline (Sigma-Aldrich) was added to the T-REx-293 cell lines for 24 hours.

Culture and treatment of human synovial sarcoma cells and MTT cell proliferation assays

Cell lines were grown in monolayer cultures and maintained at 37°C in a humidified 5% CO_2 atmosphere as described (20). Because of their low proliferative rate, HS-SY-II synovial sarcoma cells were not suitable for further functional assays. For proliferation assays, cells were cultured in medium supplemented with 2% FBS in 96-well dishes at least in triplicate. Cell density was 5×10^3 per well. Cells were exposed to increasing concentrations of dasatinib (0.01–10 μmol/L; Santa Cruz Biotech), and appropriate controls were included. For combination treatments with chemotherapeutic drugs, cell lines were incubated with increasing concentrations of doxorubicin, vincristine, and actinomycin D (0.1–100 ng/mL), alone or in combination with dasatinib in a concentration resulting in growth inhibition of 20% to 30%. Synergy was evaluated by the fractional product method (29). A difference of more than 10% between the observed and the predicted effect was considered to signify synergistic activity between dasatinib and the chemotherapeutic drug, a difference of less than 10% was defined as additive. All assays were conducted for 72 hours. MTT proliferation assays (Roche) were conducted according to the manufacturer's instructions. The formazan dye was quantified using a scanning multiwell spectrometer (BGM Labtech).

Published OnlineFirst April 15, 2013; DOI: 10.1158/0008-5472.CAN-12-3023

Knockdown of SRC and IGF-IR by RNA interference

1273/99 and CME-1 cells were cultured in 25-cm^2 flasks in medium supplemented with 10% FBS as described above. At a cell density of 50%, cells were transfected with 60 pmol Stealth RNAi (SRC: HSS186080, HSS186081, HSS186082; IGF-IR: HSS105253, HSS105254, HSS179797; Invitrogen) or nontargeting control siRNA (Invitrogen) using Lipofectamine RNAiMAX (Invitrogen) according to the manufacturer's instructions. After 24 hours, cells were trypsinized, reseeded, and MTT assays were conducted as described above (2% FBS). To document SRC knockdown, 5×10^4 siRNA-transfected cells were plated in 12-well dishes in medium supplemented with 2% FBS and cultured for 72 hours.

Western blot analysis

A total of 2×10^5 to 4×10^5 cells were seeded in 6-well dishes (Greiner) in medium supplemented with 2% FBS for 48 hours before treatment with increasing doses of dasatinib for 60 minutes. To document SRC activation via the IGF-IR pathway, 1273/99, FUJI, and CME-1 cells were starved for 4 hours and treated with 200 ng/mL recombinant IGF-II (R&D Systems). Cell lysis and Western blots were conducted as described before (20). Following primary antibodies were used according to the manufacturer's instructions: β-actin (Sigma-Aldrich), c-SRC (Santa Cruz Biotech), p-(Tyr416)-SRC, p-(Tyr527)-SRC, STAT3, p-(Tyr705)-STAT3, FAK, p-(Tyr576/577)-FAK, p44/42 MAPK, p-(Thr202/Tyr204)-p44/42 MAPK, AKT, p-(Ser473)-AKT, IGF-IR, p-(Tyr1131/Tyr1146)-IGF-IR (all Cell Signaling Technologies), CSK, and PTP1B (Abcam). Secondary antibody labeling as well as filter development were conducted using the ECL kit (Amersham) as described before (26).

Flow cytometry

About 8×10^5 cells were grown in 75-cm^2 cell culture flasks in medium supplemented with 2% FBS. After a preincubation of 18 hours, they were treated with 0.1 or 0.6 μmol/L dasatinib for 48 hours. For flow cytometric immunophenotyping, 1×10^6 cells were fixed on ice in ice-cold 2% paraformaldehyde for 10 minutes. They were then washed in PBS, collected by centrifugation, resuspended and incubated in ice-cold PBS with 0.25% Triton X-100 for 5 minutes on ice. After another washing step, cells were resuspended in 100 μL PBS/0.5% bovine serum albumin (BSA) containing an Alexa Fluor 647–labeled phospho-(Ser10)-histone H3 antibody (Cell Signaling Technology; 1:20) and a phycoerythrin-labeled cleaved PARP (Asp214) antibody (BD Biosciences; 1:5) and incubated for 30 minutes at room temperature. After an additional washing step, 500 μL PBS containing 10 μg/mL 4′,6-diamidino-2-phenylindole (DAPI; Sigma-Aldrich) was added to stain DNA, and cells were incubated for an additional 30 minutes at room temperature. Analysis was conducted using a three-laser LSRII analytical flow cytometer (BD Biosciences). Each experiment was carried out at least in duplicate. At least 30,000 events were recorded per experiment. Only single cells were included in the analysis. Data were analyzed using FlowJo (Tree Star) analysis software. To document SRC specificity of the effects of dasatinib, the experiment was additionally carried out in CME-1 cells 48 hours after SRC siRNA transfection, which was done as described above.

Analysis of apoptosis by DAPI staining

Cells were cultured as described above and treated with 0.03 or 0.3 μmol/L dasatinib. They were harvested and washed in PBS, fixed in 3.7% paraformaldehyde for 10 minutes at room temperature, and washed again. After incubation with 1 μg/mL DAPI (Sigma-Aldrich) for 10 minutes and 2 further washing steps, cells were mounted on appropriate slides using Fluoromount-G medium (Southern Biotechnologies Associates). Nuclei were visualized and photographed using a Leica DMLB fluorescence microscope. Apoptotic cells were morphologically defined by chromatin condensation and fragmentation. For each assay, at least 300 cells were analyzed in triplicate.

Wound scratch, migration, and invasion assays

Cellular motility, migration, and invasion were analyzed by wound scratch, Boyden chamber, and invasion chamber assays. To exclude influences of growth effects on the results of migration and invasion assays, dasatinib was used in concentrations of 1 or 3 nmol/L, that is concentrations, which were shown to exert no significant effects on cell viability in MTT assays. CME-1 and SYO-1 cells were grown to confluence in 6-well dishes under serum-reduced conditions as described above. Cell monolayers were wounded by scratching with a sterile 100-μL pipette tip, medium was exchanged and the cells were treated with dasatinib or dimethyl sulfoxide (DMSO) as control. Photographs were taken at time points 0, 12, and 24 hours, using an AxioCam digital camera and the AxioVision software (Zeiss). Boyden chamber motility assays were conducted with CME-1, SYO-1, and 1273/99 cells. A total of 2×10^4 to 7×10^4 tumor cells in 150 μL medium containing 2% FBS were added into the upper Transwell chambers (6.5-mm diameter, 8.0-μm pore size, Corning Costar Corporation) and treated with dasatinib or DMSO as control for 24 hours. FBS concentration in the lower chamber (500 μL) was 10%. Invasion chambers with Matrigel coating (6.4-mm diameter, pore size 8 μm; BD) were used to assess the effect of dasatinib on invasion in CME-1 and SYO-1 cells. Essentially, cells were seeded and treated as for migration assays. Dishes were incubated in a 37°C incubator (5% CO_2) for 24 hours. After removal of the nonmigrating cells from the upper chamber with a cotton swab, the membranes were fixed with 4% paraformaldehyde for 15 minutes, stained with Harris hematoxylin for 15 to 20 minutes, washed, removed from the plastic holders, and mounted on glass slides with Aquatex (Merck). Migrated cells were counted in five ×10 fields (×100 magnification). All assays were conducted at least in triplicate. To document SRC specificity of the effects of dasatinib, Boyden chamber and invasion chamber assays were additionally conducted in CME-1 cells 48 hours after SRC siRNA transfection, which was done as described above.

RhoA and Rac activation assay

CME-1 and SYO-1 cells were cultured as described above to yield a density of 30% to 60% after 72 hours. Cells were

Published OnlineFirst April 15, 2013; DOI: 10.1158/0008-5472.CAN-12-3023

then treated with 0.1 μmol/L of dasatinib for 20 minutes. DMSO was used as control. Lysates were prepared and immediately snap-frozen in liquid nitrogen. Protein lysates with equalized concentrations were analyzed. The assay was conducted in duplicate according to the manufacturer's instructions (Cytoskeleton).

In vivo experiments in SYO-1 xenografts

All mouse procedures were conducted in accordance with the National and European Union guidelines and permission was obtained from the local authorities. A total of 5×10^6 SYO-1 synovial sarcoma cells were injected subcutaneously into the right flank of 5-week-old BALB/c nude mice (Charles River Laboratories). Tumor growth was assessed daily by measuring the tumor volume calculated as length × width × height × $\pi/6$. Treatment was started when the tumor volume reached 100 mm^3. Dasatinib was injected intraperitoneally (i.p.) in a daily dosage of 10 mg/kg (days 1–7). As no side effects were observed during the first week of treatment, the dosage was escalated to 20 mg/kg (days 8–14). After 15 days of treatment, animals were sacrificed, tumors were explanted, and the tumor tissue was formalin-fixed and embedded in paraffin.

Results

Phosphokinase arrays

Phosphokinase array analysis of 1273/99 and HS-SY-II synovial sarcoma cells detected phospho-(Tyr416)-SRC as the most strongly phosphorylated protein kinase of 46 represented targets. Independent Western blotting confirmed this finding and detected p-(Tyr416)-SRC levels of different intensity in CME-1, SYO-1, FUJI, 1273/99, and HS-SY-II synovial sarcoma cells (Fig. 1; Supplementary Table S1). Because of their low proliferative rate, HS-SY-II synovial sarcoma cells were not suitable for further functional assays.

Synovial sarcomas display elevated levels of Tyr416-phosphorylated SRC

In a set of 30 synovial sarcomas, immunohistochemical stainings revealed strong expression levels of Tyr416-phosphorylated SRC in 13% of the samples, 60% showed moderate, and 27% weak expression levels. In contrast, strong Tyr527-phosphorylated SRC was detectable in only 7% of the samples, whereas moderate or weak expression was found in 10% and 30% of the tumors, respectively; in 53% of the samples, no

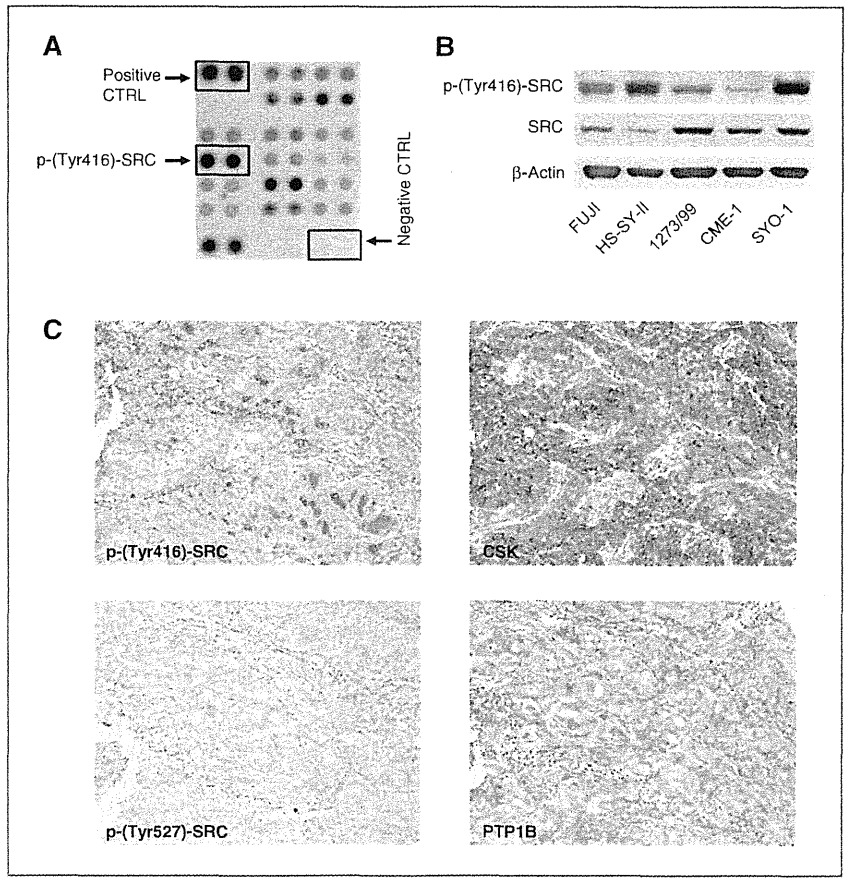

Figure 1. A, Tyr416-phosphorylated SRC was found to be the most strongly phosphorylated kinase in a phosphokinase array analysis of 1273/99 synovial sarcoma cells. B, expression of p-(Tyr416)-SRC was confirmed by Western blot analysis. C, representative case of a biphasic synovial sarcoma displaying high expression of p-(Tyr416)-SRC, weak expression of p-(Tyr527)-SRC, high CSK levels, and weak PTP1B expression.